A Study of Estuarine Tidal Dissipation and Bottom Stress

UNH Sea Grant
Technical Report UNH-SG-166

A STUDY OF ESTUARINE TIDAL DISSIPATION AND BOTTOM STRESS

Richard P. Trask
and
Wendell S. Brown

Report No: UNH-SG-166

Department of Earth Sciences
University of New Hampshire
Durham, New Hampshire 03824

February 1980

This publication is a result of research sponsored by the NOAA office of Sea Grant, Department of Commerce. The U.S. Government is authorized to produce and distribute reprints for governmental purposes not withstanding any copyright notation that may appear here on.

TABLE OF CONTENTS

LIST OF TABLES		v
LIST OF FIGURES		vi
ABSTRACT		vii
CHAPTER I	INTRODUCTION	1
CHAPTER II	1978 FIELD PROGRAM	11
CHAPTER III	RESULTS	15
CHAPTER IV	DISCUSSION AND CONCLUSIONS	30
REFERENCES		35
APPENDIX A	THE ENERGY DISSIPATION CALCULATION	36
APPENDIX B	THE ENERGY DISSIPATION DUE TO VERTICAL MIXING CALCULATION	43
APPENDIX C	INSTRUMENT DEPLOYMENTS	46
APPENDIX D	UNCERTAINTY ESTIMATES	50
APPENDIX E	CHARACTERISTIC VELOCITY CALCULATION	56
APPENDIX F	TIDAL PRISM VOLUME DETERMINATION	60

LIST OF TABLES

1. Preliminary energy budget results..... 9

2. A summary of the bottom stress calculation results..... 29

3. A comparison of the tidal energy dissipation occurring in Great Bay Estuary, Narragansett Bay and the Bay of Fundy..... 31

4. A summary of the high and low water areas and the calculated volumes..... 63

LIST OF FIGURES

1. A schematic of a constant section estuary showing the dimensions referred to in Taylor's energy flux equation..... 3

2. Map showing the location of the preliminary study area in the Great Bay Estuary..... 7

3. Map showing the location of the area of interest in the 1978 field program..... 12

4. Time series of volume transports which have been normalized to a tidal range of 2.0 meters..... 17

5. A summary of data acquisition during the 1978 field program..... 20

6. Data used in the bottom stress calculation..... 22

7. Components of the bottom stress calculation..... 23

8. Predicted sea level, sea level difference and velocity for the study area..... 25

9. Bottom stress and the component terms based on the 30 day predictions in figure 8..... 27

10. Typical cross-sections from both ends of the study area..... 37

11. A plot of the long-channel component of current velocity versus volume transports from the upstream transect..... 39

12. A plot of the long-channel component of current velocity versus volume transports from the downstream transect..... 40

13. A summary of the procedure used to calculate the energy dissipation within the study area..... 42

14. A schematic drawing of the tripod anchor frame..... 47

15. A schematic drawing of the locations of the two pressure sensors and the Geodyne current meter in the center of the channel..... 49

16. A sequence of current profiles measured near the Geodyne current meter on 21 September 1978..... 57

17. A comparison of depth averaged velocity from current profile measurements and the predicted bottom currents based on the tidal analysis of the Geodyne currents..... 58

18. The Great Bay Estuary with the longitudinal estuarine scale..... 61

19. Schematic representation of a tidal prism volume in an estuary..... 62

A STUDY OF ESTUARINE TIDAL DISSIPATION AND BOTTOM STRESS

Richard P. Trask
and
Wendell S. Brown

Department of Earth Sciences
University of New Hampshire
Durham, New Hampshire 03824

ABSTRACT

Estimates of bottom stress in a tidal estuary have been made by two independent means. Net energy budget calculations provided estimates of rates of tidal energy dissipation which can be interpreted in terms of an area averaged bottom stress (energy dissipation method). A second independent estimate of an area averaged bottom stress was made using the long-wave momentum and continuity equations and estimates of sea surface slope and current acceleration (dynamic inference method). Preliminary energy budget calculations made for the Great Bay Estuary, New Hampshire, showed that a two kilometer section of the estuary exhibits anomalously large tidal energy dissipation which we assume is due to bottom friction. Therefore a field program designed to acquire current velocity and bottom pressure data was conducted in the high dissipation region. Current profiling was conducted for a tidal period at each end of the study area. These data provided input into an energy budget calculation. The average energy dissipation per unit area for the study region is 4940.0 ± 2519 ergs/cm^2/sec as com-

pared with an average value of 390 ± 28 ergs/cm^2/sec for the entire estuary. Using the energy dissipation method an area averaged bottom stress for the study area was calculated to be 80.5 ± 41 dynes/cm^2.

Estimates of sea surface slope were obtained using bottom pressure sensors at either end of the study area. The difference between the bottom pressures was interpreted as the fluctuating part of the sea surface slope. A representative current was obtained from a mid-channel site between the pressure measurements for the determination of the flow acceleration. Since the bottom pressure series overlapped for only 2 days at a time of neap tides the bottom stress estimate obtained by using the dynamic inference method gave an area averaged bottom stress of 45.94 ± 5.05 dynes/cm^2. A bottom stress obtained by using the dynamic inference method with 30 days of predicted sea level and current data gave a bottom stress of 55.28 ± 6.47 dynes/cm^2.

CHAPTER I

INTRODUCTION

This study was designed to develop a tidal energy balance for a section of the Great Bay Estuary in southeastern New Hampshire. The energy balance consists of the net flux of tidal energy into the study area and the dissipation of that energy due to vertical mixing and bottom friction. Since bottom friction is a difficult quantity to measure directly it has been determined here by taking the difference between the net flux of tidal energy into the estuary and the rate of dissipation within the estuary due to vertical mixing.

Since frictional energy dissipation is proportional to the square of the current speed (Filloux, 1973), large dissipation rates from the deep ocean bottom, where current measurements are low, seem unlikely. Therefore coastal dissipation is the most likely energy sink. Estimates of tidal energy dissipation rates for the world's oceans and coastal regions suggest that a large amount of tidal energy dissipation occurs in coastal areas. Hendershott and Munk (1970) have calculated a tidal energy dissipation rate for the world's oceans of 2.7×10^{19} ergs/sec based on an observed rate of acceleration of the moon. Jeffreys (1921) calculated a similar dissipation rate of 2.2×10^{19} ergs/sec using coastal tidal observations. Miller (1966) estimated that $1.7 \times 10^{19} \pm 50\%$ ergs/sec of world's ocean's dissipation occurs in coastal regions and shallow seas. The large uncertainty in this estimate is related to the relatively sparse set of observations and a limited understanding of frictional processes which lead to

energy dissipation. Detailed studies in shallow seas can help our understanding of dissipation processes and add to the sparse set of observations.

Several attempts have been made to estimate the dissipation of tidal energy in specific coastal bodies of water. One pioneering effort was made by Taylor (1919) who calculated the energy flux into a region by adding estimates of work done by hydrostatic pressure to those due to the flux of gravitational potential energy and kinetic energy. He expressed the time averaged rate of energy flux through a bay passage, W_F, as follows:

$$W_F = < \rho \, g \int h \, \eta \, U \, dy > \qquad (1)$$

where U is the long-channel current, h is the depth of the bottom below mean sea level, η is the height of the tide above mean sea level, ρ is the density of sea water, g is the acceleration due to gravity, dy is an increment of length across the channel and < > indicates a time average. The dimensions these terms refer to are shown in figure 1.

Taylor (1919) presents an energy budget in which the average rate of energy flux, W_F, into a region is equal to the average rate at which that energy is dissipated by tidal friction, W_D, minus the average rate at which work is done on the region by the moon's attraction, W_M. According to Taylor the moon's gravitational attraction on the body of water imparts energy into the system. The contribution of that energy has to be subtracted in order to balance the energy budget. Thus the dissipation of tidal energy can be estimated from the following equation:

$$W_D = W_F + W_M \qquad (2)$$

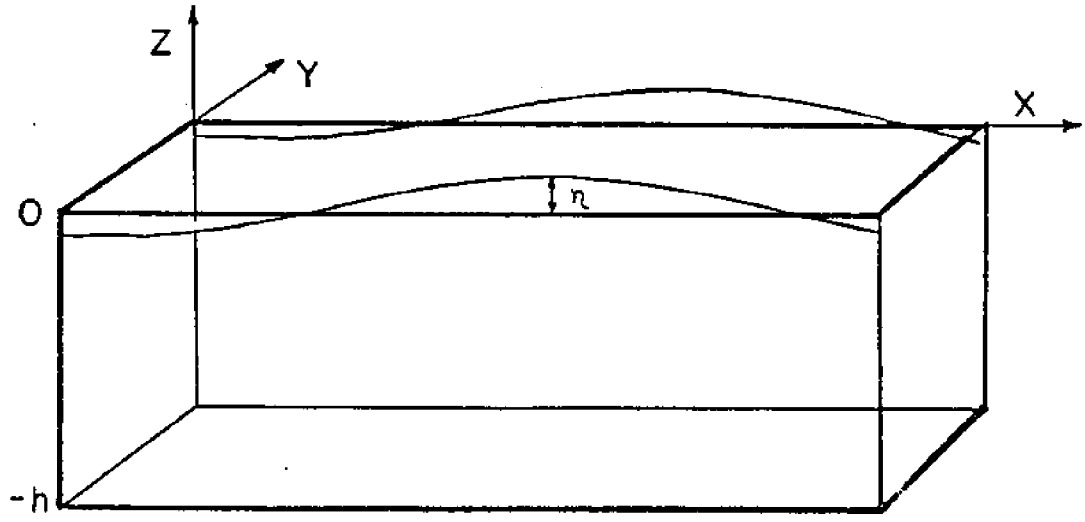

FIGURE 1. A schematic of a constant section estuary showing the dimensions referred to in Taylor's (1919) relationship for calculating a time averaged rate of energy flux.

McLellan (1958) included an additional energy sink term associated with vertical mixing, W_{MIX}, in his energy balance for the Bay of Fundy. In his work, the homogeneity of the water column in that area was attributed to the vertical mixing action of the tides. Since the water in the Great Bay study area is also well mixed vertically this energy dissipation factor was therefore included in Taylor's original energy balance equation to give the following equation:

$$W_D = W_F + W_M - W_{MIX} \tag{3}$$

McLellan defines W_{MIX} as the difference between the potential energy in a column of homogeneous sea water of depth $\eta + h$, (PE), which is found according to:

$$(PE) = \int_0^{\eta + h} \rho\, g\, (h + z)\, dz \tag{4}$$

and the potential energy for an ideal situation of an unmixed fresh water layer and a salt water layer, (PE)', which is found according to:

$$(PE)' = \overline{(h + z_s)}\ \Delta z_s\ \rho_s g + \overline{(h + z_f)}\ \Delta z_f\ \rho_f g \tag{5}$$

where Δz_s is the thickness of the salt water layer, $\overline{(h + z_s)}$ is the mean height of the salt water layer, Δz_f is the thickness of the fresh water layer and $\overline{(h + z_f)}$ is the mean height of the fresh water layer. A more detailed description of this calculation appears in Appendix B.

Previous studies by McLellan (1958) and Levine and Kenyon (1975) have calculated energy budgets according to equation (3). The results of Levine and Kenyon's energy balance for Narragansett Bay showed that 73% of the total tidal energy dissipation was in the form of frictional dissipation, 15% was due to work done on the moon and the remaining 2%

was due to dissipation from mixing. McLellan (1958) found for the Bay of Fundy that approximately 91% of the total tidal energy dissipation was due to friction, 8% was due to work done on the moon and .1% was due to vertical mixing.

More recently Garrett (1975) has derived a general energy balance for a gulf from the long-wave equations of motion. His work shows that Taylor had failed to account for the flux of "equilibrium" energy out of the gulf and in fact the sum of the omitted term and the term Taylor did include, W_M, is much less than either of the individual terms. Thus Taylor's energy budget overestimates the effect of the astronomy and the following adjustment to equation (3) is made.

$$W_D = W_F - W_{MIX} \tag{6}$$

If the rate of energy dissipation within a section of an estuary is desired then a modified form of equation (6) is applicable. W_F is replaced by the difference between the average energy flux value for the downstream end of the study area, W_{F1}, and the average energy flux value for the upstream end, W_{F2}, such that

$$W_D = (W_{F1} - W_{F2}) - W_{MIX} \tag{7}$$

The difference in energy flux values, $(W_{F1} - W_{F2})$, is the average rate of energy dissipation within the section. For future reference the average rate of energy dissipation will be represented by the symbol Φ with units of ergs/sec, whereas the average dissipation rate per unit area will be represented by the symbol ϕ with units of ergs/cm^2/sec.

We have made a preliminary energy budget calculation based on equation (7) using data collected during the summer of 1975. The 1975

field program was designed to investigate the vertical and lateral variability of the currents within the Great Bay Estuary with a series of thirteen hour current transects. For the energy budget calculation we chose the two located at each end of a four kilometer section of the lower Piscataqua River as shown in figure 2. One transect was occupied on August 5, 1975, near Frankfort Island while the other was made near Portsmouth, New Hampshire, on September 24, 1975. Each transect consisted of three stations spaced across the channel. A current velocity profile was measured at each station using a Marsh McBirney model 727 electromagnetic water current meter. Additional details of the field program and the equipment used are described by Swenson, Brown and Trask (1977).

In addition time series data of current velocity was collected by the National Ocean Survey (NOS) at each end of the study area. The time series records coincided for fourteen days from July 26, 1975 to August 9, 1975. The use of the current time series in the time averaging calculation will be discussed next.

The accuracy of an energy flux calculation is sensitive to the time averaging procedure. In our case the existence of a significant diurnal inequality leads to poor results when averaging only thirteen hours of current data. We have addressed this question by first estimating thirteen hourly values of volume transport and then finding a regression relationship between the transport and the time series of current velocity. That relationship was assumed to apply for longer periods and was used to produce a fourteen day time series of volume transport. The transport time series and (1) and (7) were used to produce a fourteen day average of energy flux. The details of this calculation are summarized in Appendix A.

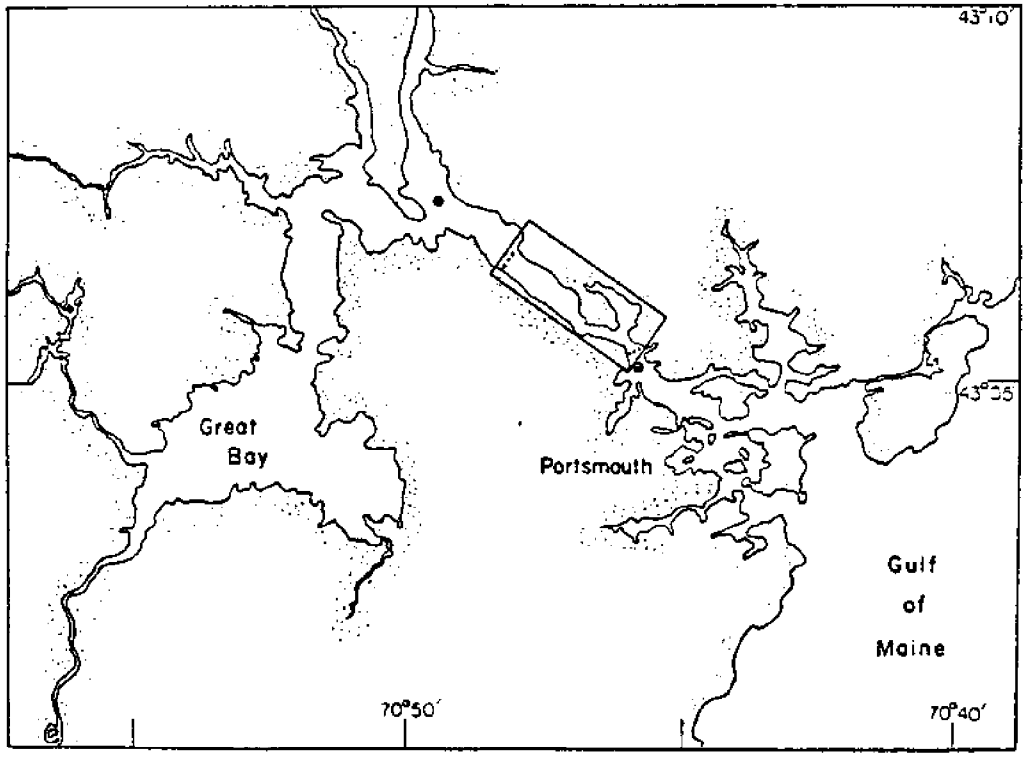

FIGURE 2. Great Bay Estuary in southeastern New Hampshire. The rectangular section outlines the area of interest in the preliminary study. The transect station locations are indicated by (•). The location of the NOS current meters used in the preliminary study are indicated by (⊛).

The results of the preliminary energy budget calculation show that the value of ϕ for the study region is nearly twenty times larger than the value of ϕ obtained for the entire estuary. According to McLellan's (1958) method for calculating W_{MIX}, a rate of dissipation of 5.02×10^{10} ergs/sec or 2.5% of the total was calculated. The details of this calculation can be found in Appendix B. Bottom friction therefore dissipates 97.5% of the total energy dissipated within the study area. For the study region ϕ is 116.8 ergs/cm^2/sec whereas for the entire estuary ϕ is 5.37 ergs/cm^2/sec. We therefore conclude that anomalously large tidal energy dissipation occurs within the study area. A comparison of the preliminary energy budget results from the study area and the entire estuary is shown in table 1.

An average tidal bottom stress can be determined from the ratio of the rate of dissipation due to bottom friction and the product of the average velocity and the area of the study region. This method of calculating bottom stress will be referred to as the energy dissipation method. Since the rate of dissipation due to bottom friction is averaged over the entire study area the calculated bottom stress is an area averaged estimate. The average bottom stress value calculated for this region is 2.12 dynes/cm^2 which appears to be much lower than expected from other considerations. Energy budget calculations are extremely sensitive to measurement uncertainty thus comparison with results obtained by independent means are useful in their interpretation.

Another method for calculating an area averaged estimate can be derived from the long-wave equations of motion with bottom friction. The finite difference form of these equations for a narrow channel can be expressed in terms of bottom stress, τ_b, as

	AREA cm^2	DISSIPATION ergs/sec	DISSIPATION / AREA $ergs/cm^2/sec$	BOTTOM STRESS ESTIMATE $dynes/cm^2$	τ_b ACCORDING TO (8) $dynes/cm^2$
STUDY AREA	1.66×10^{10}	1.94×10^{12}	116.8	2.12	35.67
ESTUARY	4.06×10^{11}	2.18×10^{12}	5.4	0.18	--

TABLE 1. Preliminary energy budget results from the study area and the entire estuary.

$$\tau_b \simeq \rho\, h \left(-g \frac{\delta \eta}{\delta x} - \frac{\delta U}{\delta t}\right) \tag{8}$$

where U is the downstream depth averaged velocity, η is the sea surface elevation, h is the mean depth, and τ_b is the downstream bottom stress. For future reference this method of calculating bottom stress will be referred to as the dynamic inference method. Estimates of sea surface slope ($\delta\eta/\delta x$) and acceleration of the current ($\delta U/\delta t$) for the preliminary study area gave a first order estimate of 35.67 dynes/cm^2 compared with a bottom stress of 2.1 dynes/cm^2 obtained using the energy dissipation method. The estimates of $\delta\eta/\delta x$ and $\delta U/\delta t$ were based on a knowledge of tidal amplitudes and phase differences between sea level and current velocity and also between sea level at each end of the study area. If we believe the results of equation (8) to first order it appears that the rate of energy dissipation due to bottom friction has been greatly underestimated in the budget calculation.

To resolve the large discrepancy in these bottom stress estimates a field program was designed to make more accurate estimates. One area averaged estimate of bottom stress was made using the energy dissipation method while another was made using the dynamic inference method with estimates of $\delta\eta/\delta x$ and $\delta U/\delta t$. The measurement program designed to provide the data needed for the two independent bottom stress calculations is described in chapter II. The results of the experiment and their uncertainties are presented in chapter III which is followed by a brief discussion of how the results of this study compare with those of others.

CHAPTER II

1978 FIELD PROGRAM

During the summer of 1978 a field program designed to acquire current velocity and bottom pressure data was conducted in a section of the Great Bay Estuary in southeastern New Hampshire. The area of interest was a two kilometer section of the lower Piscataqua River between Frankfort Island and the Newington Station power plant. The study area was selected because it has been shown in chapter I to have anomalously high dissipation, it has a relatively uniform geometric configuration and there are previously collected sea level and current velocity data available from that area.

The field program consists of two parts. The first part was designed to acquire current data to be used for purposes of estimating bottom stress according to (1) and (7). The second part of the experiment was designed to provide data for purposes of estimating bottom stress according to (8).

To address the needs of part one, current velocity profiling was conducted at each end of the study area. The sampling procedures were similar to those used for data collection in the preliminary study where profiles were made at several stations within the channel for thirteen hours. A description of those procedures appears in chapter I. One transect was occupied on August 22, 1978, near the Newington Station power plant and the other was made near Frankfort Island on August 29, 1978. The location of the study area and the details of each of the transects are shown in figure 3.

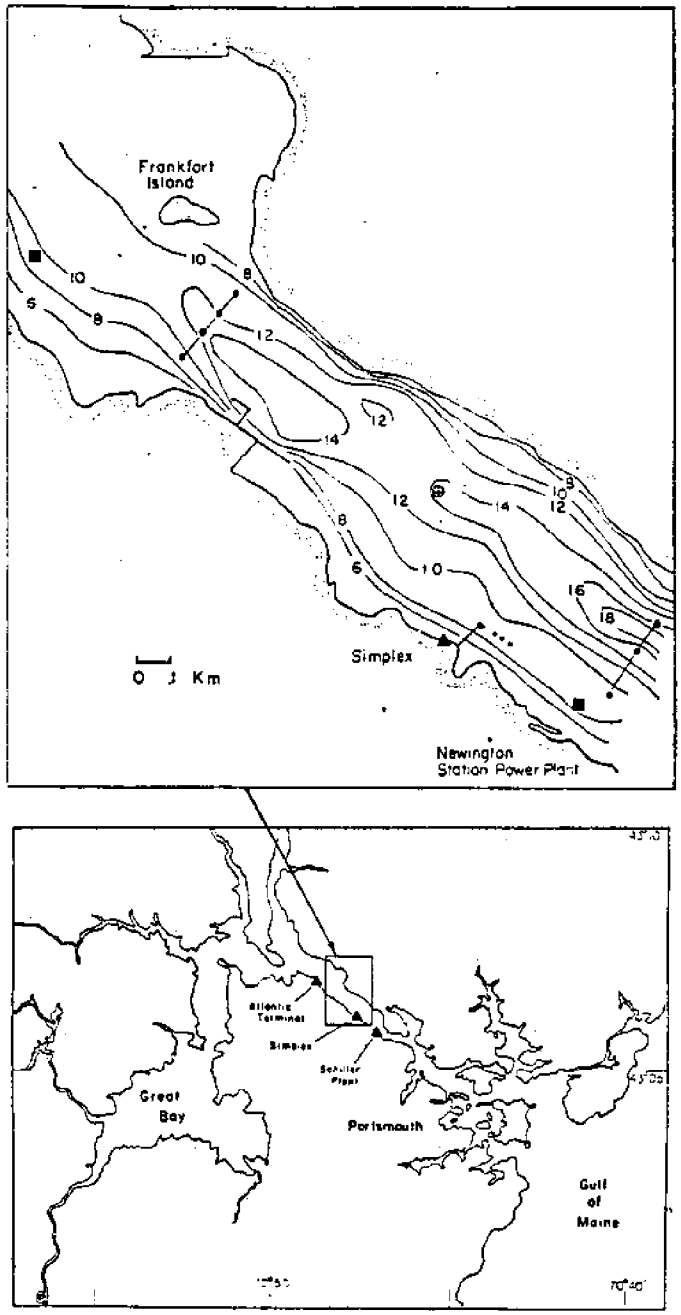

FIGURE 3. The lower map shows the Great Bay Estuary. The outlined region is the area of interest in the 1978 field program. Locations of the NOS tide stations (▲), the transect station locations (•), the current meter location (⊗) and the pressure sensor locations (■) are shown. The contour interval is two meters.

Estimates of $\delta\eta/\delta x$ and $\delta U/\delta t$ were provided by measurements made in connection with part two which are summarized here. A more detailed description of the array deployments appears in Appendix C. To estimate sea surface slope $\delta\eta/\delta x$, bottom pressure was measured on the ten meter isobath at each end of the study area. The Digiquartz depth sensors used for these measurements are capable of resolving millimeter changes of water elevation and typically have long term drift rates of less than one centimeter per month. In addition temperature measurements were made by a thermistor mounted in the pressure housing. The data was recorded by a data logging system which consists of electronics and digital cassette tape recorder. The depth sensor and the data logging system were mounted on a rigid aluminium frame and attached to a heavy anchor.

The pressure instrument "KIWI" was deployed on August 16, 1978, and retrieved on September 26, 1978. The other pressure instrument "PICKET" was deployed on August 25, 1978, and retrieved on September 26, 1978.

Current velocity data needed to estimate $\delta U/\delta t$ were acquired at the same time as the pressure measurements and current profiling. A Geodyne model 102 film recording current meter with a savonius rotor and vane was deployed between August 22 and September 21, 1978 at the site shown in figure 3 on the fifteen meter isobath. The rotor was 75 centimeters above the bottom.

A series of current velocity profiles were made at the location of the Geodyne current meter in order to determine a relationship between the near bottom Geodyne currents and the currents at higher elevation above the bottom. A series of profiles, each of which took

about fifteen minutes were obtained for the period from about two hours before low slack water to about one hour after low slack water. This period exhibits the full range of tidal currents at this location.

CHAPTER III

RESULTS

The results of the bottom stress calculations made using the energy dissipation and dynamic inference methods will be discussed next. As described in chapter I the energy dissipation method requires accurate estimates of volume transport. An estimate of the accuracy of the transports calculated from the data of the 1978 field program will be made by comparing them with estimates which are based on a knowledge of the tidal prism. However before that comparison can be made we will evaluate the uncertainty associated with averaging over a semidiurnal tidal cycle in the presence of a significant diurnal inequality. The results of the energy budget will then be presented along with an estimate of bottom stress made using the energy dissipation method. This will be followed by several estimates of bottom stress calculated using the dynamic inference method with both real and predicted data.

Since the transect data from both ends of the study area were not obtained simultaneously they had to be adjusted for the spring-neap tide differences before being compared. The downstream transect occurred at a time very close to the spring tide which had relatively strong tidal currents and a tidal range of 2.94 meters. The upstream transect took place seven days later at a time close to the neap tide which had relatively slower currents and a tidal range of 1.50 meters. In order to compare the transport values from each end of the study area both sets of results were normalized to an average tidal range of 2.0 meters. This was accomplished by multiplying the transport values

of a particular transect by the ratio of a tidal range of 2.0 meters and the tidal range on the day of the transect. The normalized transport for both the downstream and upstream transects are shown in figure 4. The difference between the ebb and flood tide transports is clearly evident. In fact an integral of the normalized volume transport curves show that 61.87 x 10^6 m^3 of water flowed through the downstream transect during the flood tide and only 50.21 x 10^6 m^3 during the following ebb tide. Similarly at the upstream transect an integral of the normalized transport curves indicates that 59.96 x 10^6 m^3 and 50.36 x 10^6 m^3 of water flowed during the ebb and flood portions of the tidal cycle respectively. An average volume of water flowing past each transect is difficult to interpret because there is only thirteen hours of transport data. Averaging over thirteen hours does not average out the effects of all of the longer period components of the tides. A thirteen hour average of the volume of water flowing past the downstream end of the study area is 56.04 x 10^6 m^3 whereas the average flow past the upstream end is 55.16 x 10^6 m^3. In order to determine the accuracy of these volume estimates they will be compared with estimates based on an independent tidal prism calculation. However before such a comparison can be made the uncertainty associated with averaging over only 12.42 hours compared with 24.84 hour averages will be evaluated by using a 24.84 hour time series of sea level with a significant diurnal inequality. Comparing the integral of the entire 24.84 hour time series with the integral of several 12.42 hour sections of the same curve shows that the 12.42 hour integrals can approximate the longer integral within ±10.7%. Thus the thirteen hour averages of the volume of water flowing past each end of the study area during a half tidal cycle have an uncertainty of ±10.7% due solely to the averaging procedure.

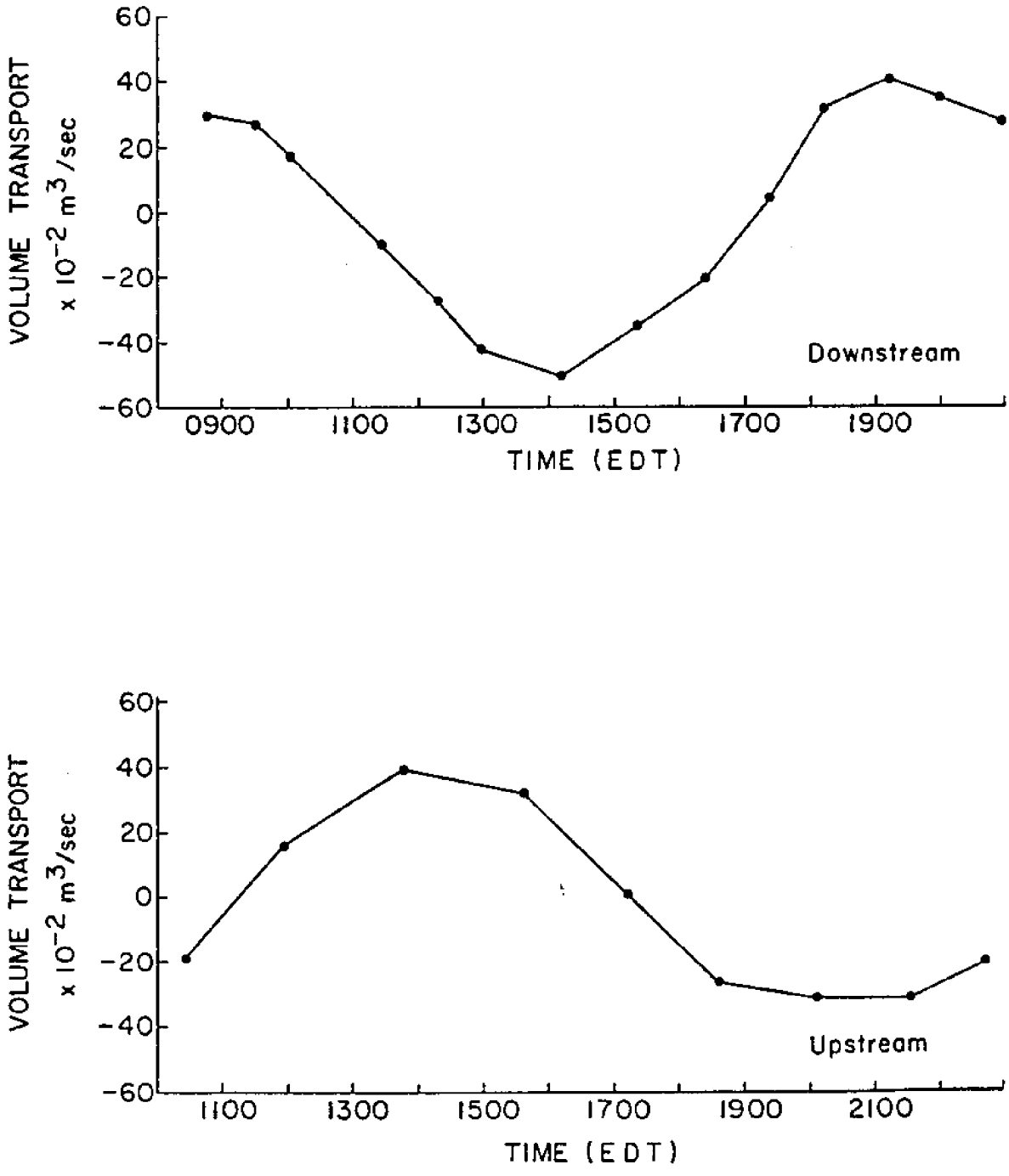

FIGURE 4. Time series of volume transports which have been normalized to a tidal range of two meters. The top plot shows downstream transport data collected on August 22, 1978, and the bottom plot shows upstream transport data collected on August 29, 1978.

The tidal prism of the estuary was determined using an average tidal range of 2.0 meters and the average water area at high and low water. According to the tidal prism calculation, 60.87×10^6 m^3 of water have to flow past the downstream end of the study area while 58.98×10^6 m^3 of water have to flow past the upstream end in order that the entire estuary have an average tidal range of 2.0 meters.

Both the upstream and downstream volumes determined from the normalized volume transport curves are low when compared with the tidal prism results by 6.48% and 7.93% respectively. This is due to averaging the transport data over only thirteen hours as well as to missing part of the flow due to the sampling procedures. For a more detailed discussion of the uncertainties introduced by the sampling procedures and other sources see Appendix D. Based on the error analysis related to the sampling procedure the volume of water flowing past the upstream and downstream ends of the study area is believed to be underestimated by 17% and 13% respectively. The error analysis of the sampling procedures and the tidal prism calculation both indicate that the volume transports have been underestimated. By averaging the percentage estimates of the amount by which the volume transports are low determined from the error analysis of the sampling procedures and the comparison with the tidal prism, the upstream and downstream transports have been estimated to be low by 11.7% and 10.5% respectively. The volume transports were therefore increased by 11% to give transport estimates which are representative of the actual flow conditions.

Applying the procedures outlined in Appendix A a fourteen day average of energy flux for the downstream end of the study area is 1.58×10^{14} ergs/sec $\pm$ 7.3% whereas for the upstream end the average energy

flux is 1.19×10^{14} ergs/sec ± 7.3%. A detailed discussion of the uncertainties related to these calculations appears in Appendix D. For the study area Φ is therefore $.395 \times 10^{14}$ ergs/sec ± 51% $(W_{F1} - W_{F2})$. The uncertainty associated with this estimate of Φ indicates the worst case. It was arrived at by applying the extremes of the uncertainties related to the average energy flux estimates in order to get the least and maximum differences for $(W_{F1} - W_{F2})$. The extreme differences varied from $.395 \times 10^{14}$ ergs/sec by ±51%.

The estimate of Φ allowed us to determine Φ and τ_b for the study region. Since the contribution of W_{MIX} was shown to be small in the preliminary study it was not considered here. For the study area Φ is 4940.0 ± 2519 ergs/cm^2/sec. In contrast Φ for the entire estuary is 390.0 ± 28 ergs/cm^2/sec. An area averaged bottom stress calculated for the study region using the energy dissipation method is 80.5 ± 41 dynes/cm^2. The procedure for calculating the characteristic velocity required for the energy dissipation method is discussed in Appendix E. This bottom stress value is considerably more than the 2 dynes/cm^2 we estimated from extremely crude historical data. We will show next that the dynamic inference method leads to bottom stress estimates of the same order as our most recent estimates.

Another method for calculating an area averaged bottom stress is by using the dynamic inference method described in chapter I. This calculation required concurrent time series of bottom pressure and current velocity. A summary of the daya acquisition during the 1978 field program is found in figure 5. The pressure instrument "KIWI" collected data between August 16 and August 27, 1978. "PICKET" the other pressure instrument recorded data between August 25 and September 26, 1978. The Geodyne current meter located in the center of the channel recorded usable data between August 22 and September 5, 1978

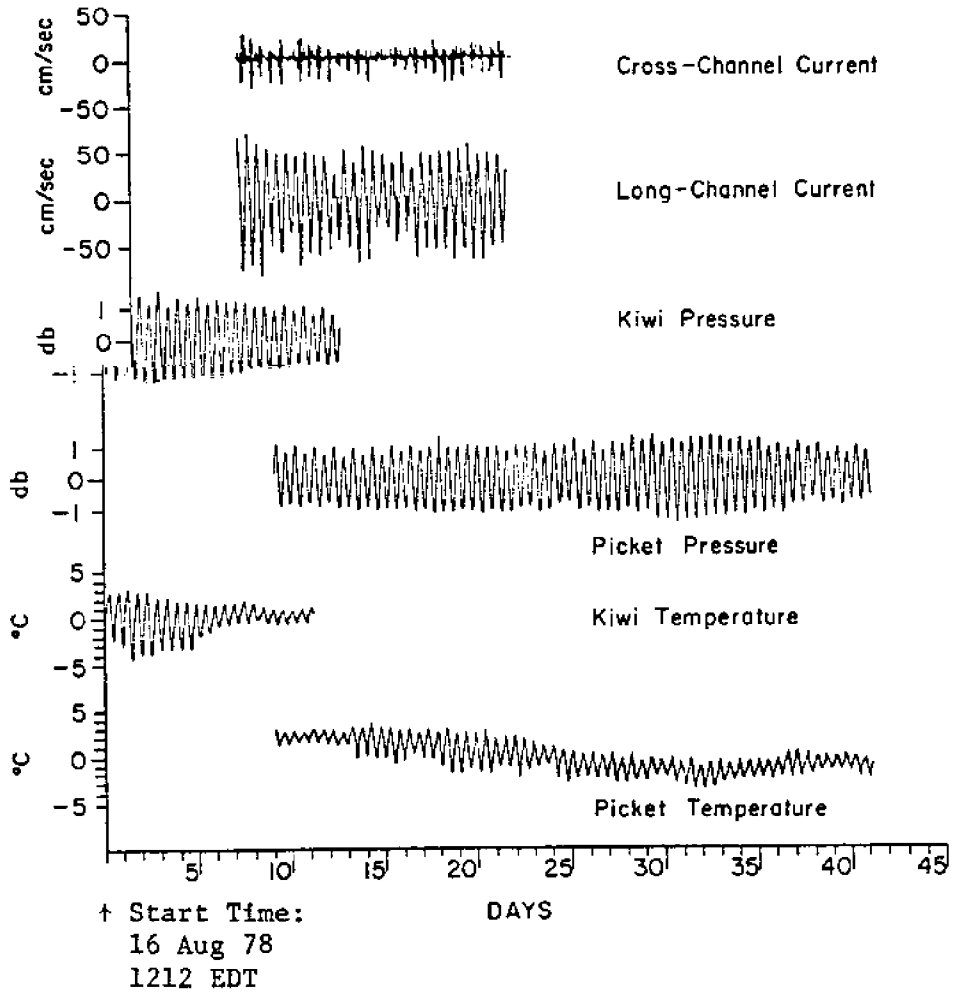

FIGURE 5. A summary of data acquisition during the 1978 field program. The mean values have been removed from the temperature and pressure series.

The goal of part two of the experiment was to estimate $\delta\eta/\delta x$ and $\delta U/\delta t$ for purposes of estimating τ_b by the dynamic inference method. Calculating $\delta\eta/\delta x$ for the study area first required removing the mean from each of the pressure series since only the fluctuations about the mean are of interest. The difference between the two pressure series was divided by the distance between the pressure sensors to give $\delta\eta/\delta x$. The current acceleration $\delta U/\delta t$ in the long-channel direction was estimated from the Geodyne current meter record. The long-channel component of current velocity U_i was converted to a depth averaged long-channel current speed $\overline{U}_i$ by using a relationship that was developed between the Geodyne current meter record and the vertical current velocity profiles made at the Geodyne current meter site. The values of $\overline{U}_i$ were first differenced and divided by the sample interval to provide an estimate of $\delta U/\delta t$.

Since the bottom pressure series overlapped for only two days bottom stress estimates from real data have been made for this period only. The data used for that estimate is shown in figure 6. The root mean square (rms) equivalent sea level difference between the bottom pressure sensors for this period was 7.55 centimeters with a corresponding rms sea level slope of 3.48×10^{-5}. The rms depth averaged current acceleration is 2.33×10^{-2} cm/sec^2. Thus with these time series estimates of $\delta\eta/\delta x$ and $\delta U/\delta t$ and using $\rho = 1.021$ gm/cm^3 and $h = 10.65$ meters equation (8) gave a rms τ_b of 45.94 ± 5.05 dynes/cm^2. Time series of current acceleration and sea level slope along with a time series of bottom stress are shown in figure 7 to display the relative importance of the different elements in this bottom stress calculation. The rms of the time series $-\rho\, h\, g\, (\delta\eta/\delta x)$ in figure 7 is 37.1 dynes/cm^2 whereas the rms of the series $-\rho\, h\, (\delta U/\delta t)$ is only 25.2 dynes/cm^2. The mean value of the acceleration term is high due to averaging noisy data obtained in the first differencing procedure. The representativeness

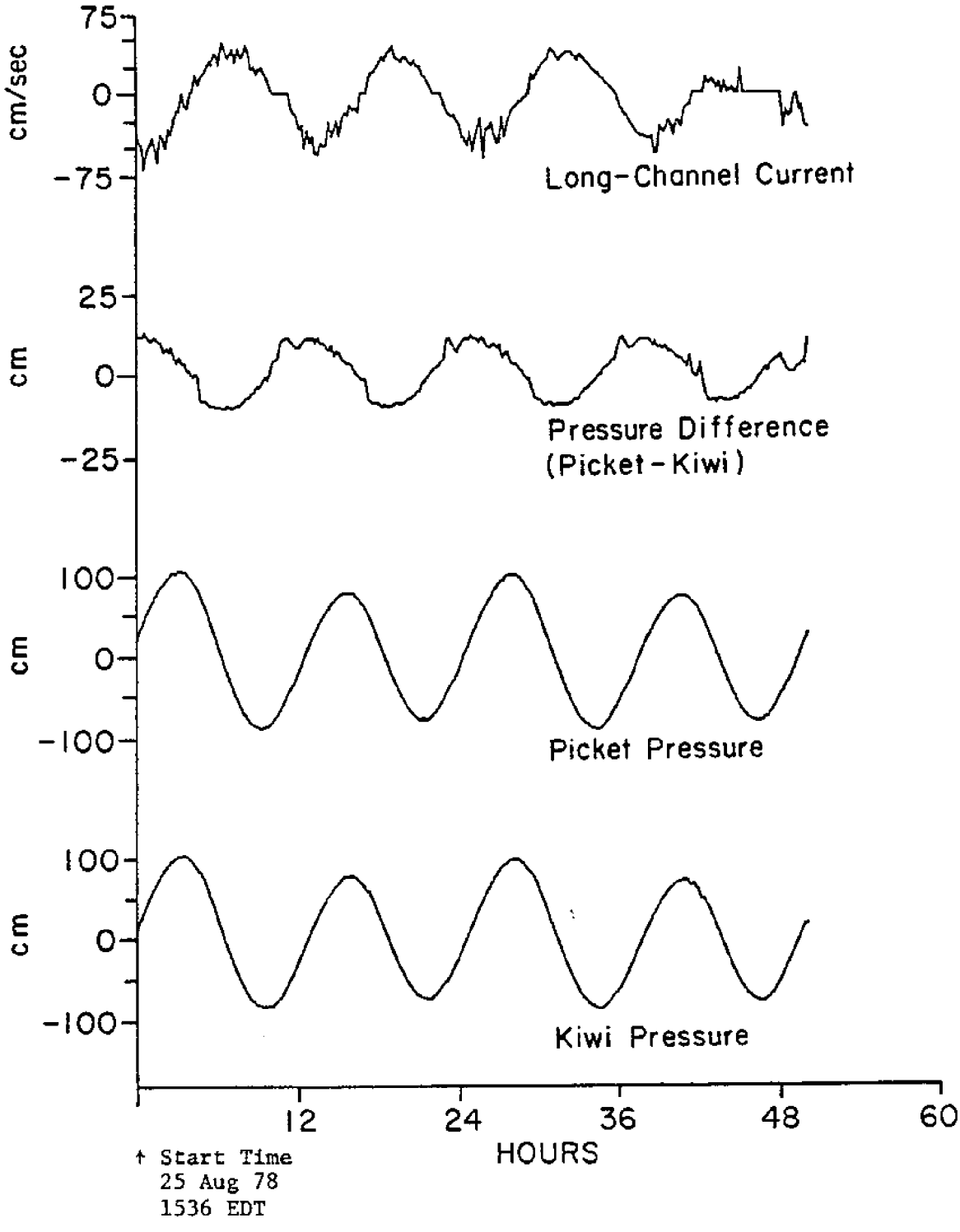

FIGURE 6. Data used in the bottom stress calculation. The pressure series have been converted to an equivalent sea level and the mean values have been removed.

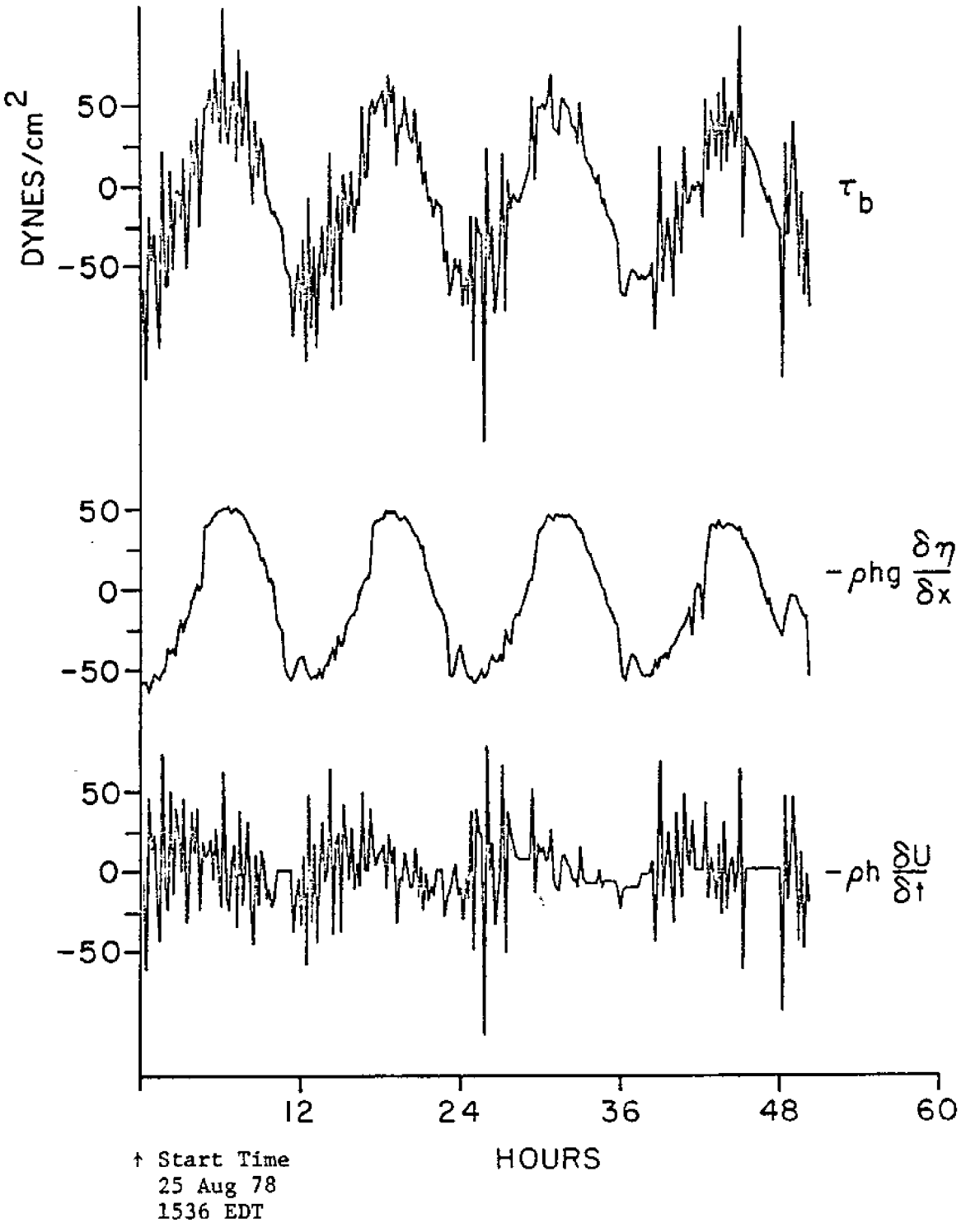

FIGURE 7. Components of the bottom stress calculation using equation (8), based on data in figure 6. The current acceleration term $-\rho\ h\ (\delta U/\delta t)$ and the sea level slope term $-\rho\ h\ g\ (\delta \eta/\delta x)$ have units of dynes/cm^2.

of this acceleration time series will be discussed later. Even with the noisy acceleration data these rms values indicate that the contribution of the pressure gradient term in (8) has a greater effect on the bottom stress than does the acceleration term.

To obtain an average τ_b over a longer period, sea level data collected by NOS in 1975 at three tide stations in the lower Piscataqua River were used to estimate $\delta\eta/\delta x$. The locations of the tide stations which are shown in figure 3 were the Atlantic Terminal dock, the Simplex Wire and Cable Company dock and the Schiller power plant. The Atlantic Terminal tide station is located upstream from the study area, whereas the Simplex tide station is near the center and the Schiller Plant tide station is located downstream from the study area. Harmonic constants for the individual tide stations were calculated using a computer program used by the NOS as outlined by Dennis and Long (1971). With the harmonic constants a predicted tide for a specified time interval at the specified station was calculated. We performed a linear interpolation between a thirty day predicted tide for the Atlantic Terminal location and a thirty day predicted tide for the Simplex location to obtain a thirty day predicted tide for the upstream end of the study area. The same procedure was used for the downstream end of the study area using predicted series for the Simplex location and Schiller power plant location. In addition the same prediction programs were applied to the current velocity. These predictions are shown in figure 8. The rms sea level difference between the ends of the study area is 10.77 centimeters which corresponds to a rms sea level slope of 4.96×10^{-5}. The rms depth averaged acceleration based on the predicted thirty day current is 8.52×10^{-3} cm/sec^2. These predictions have been

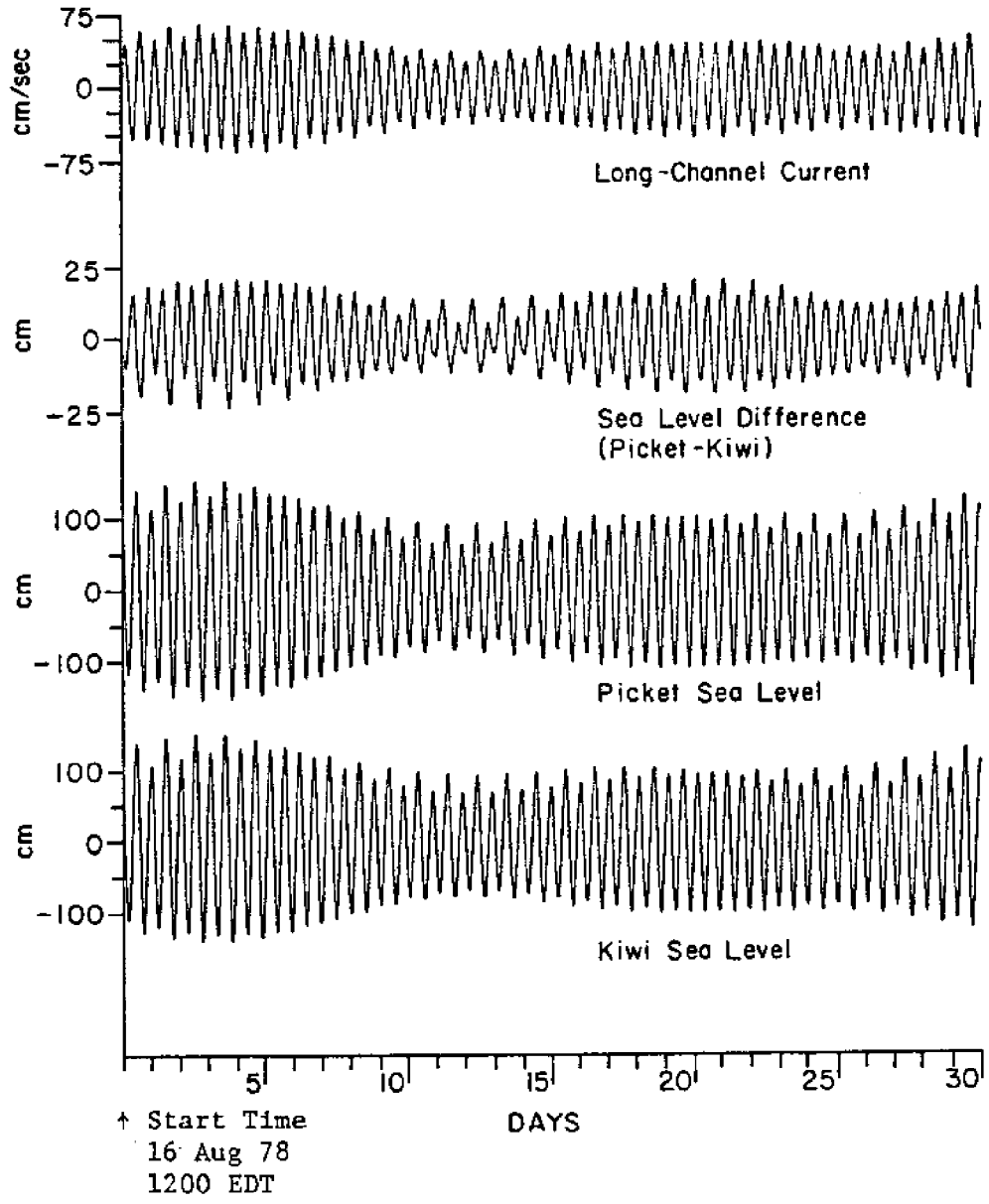

FIGURE 8. Predicted sea level, sea level difference and velocity for the study area. The velocity prediction is based on the current meter record and the sea level predictions are interpolated results from the NOS sea level stations along the study area.

used with (8) to calculate τ_b. The resulting rms bottom stress is 55.28 ± 6.08 dynes/cm^2. Figure 9 shows the relative contributions of sea level slope and current acceleration to the bottom stress. From this plot it is obvious that the bottom stress is due principally to the effects of the fluctuating pressure gradients.

A bottom stress was calculated using predicted data for a two day period which coincided with the two day overlap in pressure data. The purpose of the calculation was to compare the real data results with those obtained using predicted data. The predicted series gave a rms bottom stress of 41.42 ± 4.85 dynes/cm^2 compared to 45.94 ± 5.05 dynes/cm^2 obtained using the real pressure data. The two estimates of bottom stress agree within the limits of their uncertainties. We conclude therefore that the bottom stress values obtained when using predicted data are a good approximation of the bottom stress that would be calculated if real data was available for that time period.

Another comparison was made between the fourteen day average of bottom stress obtained using the energy dissipation method and a bottom stress calculated using the dynamic inference method with predicted data for the same time period. The dynamic inference method gave a rms bottom stress of 50.86 ± 5.95 dynes/cm^2 compared with 80.5 ± 41 dynes/cm^2 obtained from the energy dissipation method.

Since the pressure sensor PICKET collected data for thirty days a bottom stress calculation was made using the thirty days of real pressure data from PICKET and predicted sea level data from the upstream end of the study area. The rms sea level difference between the two ends of the study area was found to be 10.69 centimeters or a rms sea level slope of 4.92×10^{-5}. Using a predicted time series of

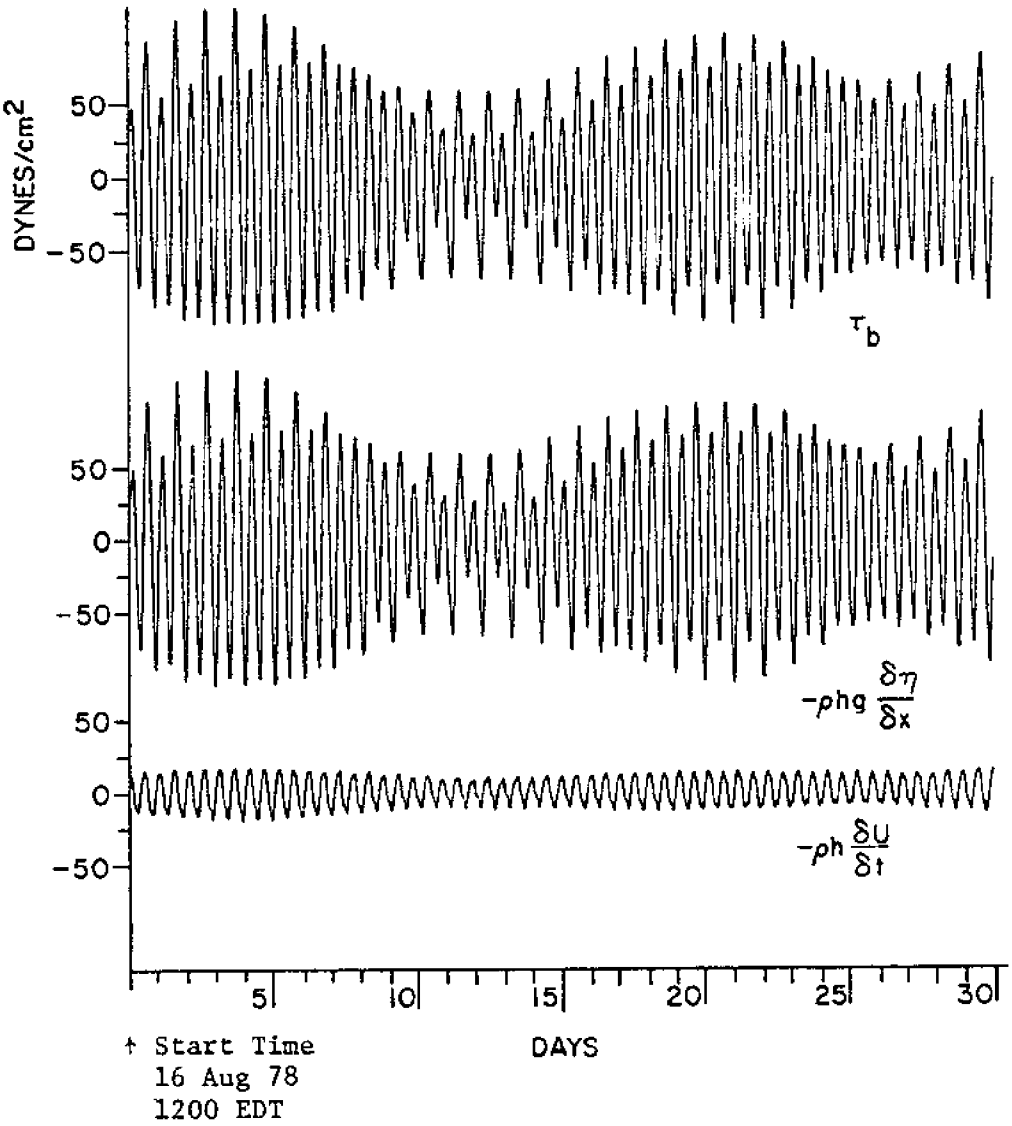

FIGURE 9. Bottom stress and the component terms based on the thirty day predictions in figure 8 and equation (8). The current acceleration term $-\rho\ h\ (\delta U/\delta t)$ and the sea level slope term $-\rho\ h\ g\ (\delta \eta/\delta x)$ have units of dynes/cm^2.

the current velocity the rms depth averaged acceleration is 8.21×10^{-3} cm/sec^2. Substituting the time series estimates of $\delta\eta/\delta x$ and $\delta U/\delta t$ into (8) gave a rms bottom stress value of 54.55 ± 6.38 $dynes/cm^2$ which can be compared with a bottom stress of 55.28 ± 6.47 $dynes/cm^2$ obtained using thirty days of predicted sea level data from both ends of the study area. A summary of the bottom stress results is found in table 2.

BOTTOM STRESS CALCULATION

	BOTTOM STRESS ($dynes/cm^2$) rms VALUES	PEAK VALUES
ENERGY DISSIPATION		
14 day average	80.5 ± 41	118.9
DYNAMIC INFERENCE		
Real Pressures and Current 2 day average (neap tide)	45.94 ± 5.05	158.2
Predicted Sea Levels and Current 2 day average (neap tide)	41.42 ± 4.85	75.9
Predicted Sea Levels and Current 30 day average	55.28 ± 6.47	118.5
Predicted Sea Level and PICKET Pressure and Predicted Current 30 day average	54.55 ± 6.38	251.7
Predicted Sea Levels and Current 14 day average	50.86 ± 5.95	105.4

TABLE 2. A summary of the bottom stress calculation results.

CHAPTER IV

DISCUSSION AND CONCLUSIONS

A number of energy budget results have been reported in the literature. Hart and Murray (1978) calculated ϕ to be 6.1 ergs/cm^2/sec for Chandeleur-Breton Sound, Levine and Kenyon (1975) 26.1 ergs/cm^2/sec for Narragansett Bay, Taylor (1919) 1300 ergs/cm^2/sec for the Irish Sea and McLellan (1958) 1880 ergs/cm^2/sec for the Bay of Fundy. The value of ϕ calculated for the Great Bay Estuary by this study is 390.0 ± 28 ergs/cm^2/sec. In contrast the two kilometer study area has a value of ϕ equal to 4940.0 ± 2519 ergs/cm^2/sec. This estimate appears to be the largest yet reported from a systematic study. The area of the study region is only 2.0% of the entire estuary however 12.6% of the total energy dissipated in the estuary occurs in the study area.

The dissipation of tidal energy which occurs in the Bay of Fundy, Narranagsett Bay and the Great Bay Estuary are shown in table 3. The value of Φ obtained for the Great Bay Estuary is 1.6×10^{14} ergs/sec whereas for Narragansett Bay and the Bay of Fundy Φ is 8.8×10^{13} ergs/sec (Levine and Kenyon, 1975) and 2.7×10^{17} ergs/sec (McLellan, 1958) respectively. These results show that the dissipation of tidal energy occurring in the Great Bay Estuary is nearly two times larger than the dissipation in Narragansett Bay. When comparing Great Bay with the Bay of Fundy we find that the Bay of Fundy dissipates more than one thousand times more energy. Thus the Great Bay Estuary plays a very minor role in the dissipation of tidal energy in the Gulf of Maine relative to the Bay of Fundy.

STUDY REGION	AREA (cm^2)	DISSIPATION / AREA ($ergs/cm^2/sec$)	DISSIPATION (ergs/sec)
Great Bay Estuary	4.06×10^{11}	390.0 ± 28	$1.6 \times 10^{14} \pm .11 \times 10^{14}$
Narragansett Bay	3.36×10^{12}	26.1	$1.1 \times 10^{14} \pm .14 \times 10^{14}$
Bay of Fundy	1.44×10^{14}	1880.0	3.0×10^{17}

TABLE 3. A comparison of the tidal energy dissipation occurring in the Great Bay Estuary, Narragansett Bay and Bay of Fundy.

The accuracy of the energy budget calculation is particularly sensitive to the difference in volume transport estimates. In this particular bottom stress calculation transport uncertainties of ±7% produced uncertainties in the bottom stress of ±51%. The entire calculation is dependent on the positions of the current velocity measurements made during the transects at each end of the study area. Extreme care must be taken to assure that the current measurements are made at locations which accurately represent the flow. A knowledge of the channel bathymetry is needed in order to position the stations in the best locations. In addition the time between successive transects must be kept to a minimum if the estimates of volume transport are to be accurate.

The relative sizes of the contributions made by the acceleration term and sea level slope is clearly shown in figures 7 and 9. The time series of bottom stress is nearly identical to the time series of sea level slope in both phase and amplitude. Thus the principal influence on the bottom stress is the pressure graduents. The acceleration term shown in figure 7 is believed to be spurious based on a comparison with the same term in figure 9.

Within the uncertainty limits of each of the bottom stress calculations there is agreement amongst the individual values. The greatest confidence lies in the bottom stress values obtained by using the dynamic inference method. Based on the nearly identical estimates of τ_b obtained using two days of real pressure data and two days of predicted data it appears that the bottom stress calculations made using predicted data can accurately estimate τ_b . In addition the calculations made over the longer time periods, for example thirty days, provide an estimate of τ_b which has been averaged over several spring -

neap tidal cycles. For this reason the thirty day rms bottom stress obtained using predicted data is believed to be a representative estimate of an area averaged bottom stress for the study area.

The difference between the two, fourteen and thirty day analysis is due to averaging over time periods which do not include all the major fluctuations in sea level and current velocity.

two day
b by 25%
though the
iffers con-
t this bottom
ng at neap

attempted
eddy vis-
several loca-
lationship
ed current
oped they
re current
ottom stress
rements.
tions within
r measurements

are:

(neap tide) value of τ_b differed from the thirty day r
whereas the fourteen day rms τ_b only differed by 8%.
two day average of τ_b calculated from real pressure da
siderably from the thirty day average we are confident
stress value is an accurate estimate of the stress occ
tide.

Another way of estimating near bottom stress has
by Swift, Reichard and Celikkol (1979) who have been u
cosity models and measurements of turbulent velocities
tions in the Great Bay Estuary. They hope to develop
between the stress measurements and the more easily me
above the bottom. Once such a relationship has been d
will be able to predict values of stress for locations
profiles have been made. The area averaged estimates
that we obtain can then be compared with their point m
Since their point measurements apply only to specific
the estuary there is a question of how representative
will be for other locations in the estuary.

In summary the results of this study of bottom st

1. An area averaged bottom stress estimate of 55.3 ± 6.5 dynes/cm^2 was obtained for the study area using the dynamic inference method. This estimate seems reasonable considering the rate of energy dissipation occurring in the study region.
2. The study area has an average rate of energy dissipation per unit area of 4940.0 ± 2519 ergs/cm^2/sec, which is the largest yet reported from a systematic study.
3. 12.6% of the energy dissipated in the entire estuary occurs over only 2% of its area.
4. From the bottom stress calculation made using the dynamic inference method it is obvious that the sea level slope has a greater effect on the bottom stress than does the current acceleration in this area of the estuary.
5. The bottom stress calculated using the energy dissipation method is particularly sensitive to the uncertainties in the estimation of volume transport. Uncertainties of ±7% in transports results in bottom stress uncertainties of ±51%.

ACKNOWLEDGEMENTS

A special thank you is reserved for Dr. M. Robinson Swift and Dr. Ronnal Reichard for their assistance with field work and critical review of this manuscript. The fruitful discussions with Dr. J. D. Irish were of great assistance in the data analysis and interpretation phase of this work. The field assistance provided by Ms. Karen Garrison, Mr. Andrew Silver, and Mr. Edward Schmidt is greatly appreciated. Mr. Paul Pelletier, captain of the R.V. Jere Chase, provided invaluable advice and assistance with the deployment and retrieval of the experimental equipment. A special asknowledgement is reserved for R. Trask's wife, Janet, who provided important moral support during the completion of this work.

This research was supported in part by the University of New Hampshire Sea Grant 4-20379-215 and by Leslie Hubbard Funds.

REFERENCES

Arellano, E., 1978: An application of a segmented tidal prism model to the Great Bay Estuarine System, M.S. Thesis, Dept. of Earth Sciences, University of New Hampshire.

Dennis, R.E. and E.E. Long, 1971: A user's guide to a computer program for harmonic analysis of data at tidal frequencies, NOAA Technical Report NOS-41.

Filloux, J.H., 1973: Tidal patterns and energy balance in the Gulf of California, Nature, 243, 217-221.

Garrett, C., 1975: Tides in gulfs, Deep Sea Research, 22, 23-35.

Hart, W.E. and S. Murray, 1978: Energy balance and wind effects in a shallow sound, J. Geophys. Res., 83(C8), 4097-4106.

Hendershott, M. and W. Munk, 1970: Tides, Annual Rev. of Fluid Mech., 2, 205-224.

Jeffreys, H., 1920: Tidal friction in shallow seas, Phil. Trans. Roy. Soc. London, Ser. A, 221, 239-264.

Levine, E.R. and K.E. Kenyon, 1975: The tidal energetics of Narragansett Bay, J. Geophys. Res., 80(12), 1683-1688.

Loder, T.C. and P.M. Glibert, 1977: Great Bay Estuarine Field Program 1975 Data Report, Part III: Nutrient Chemistry, UNH Sea Grant Technical Report, UNH-SG-159, 1-113.

McLellan, H.J., 1958: Energy considerations in the Bay of Fundy system, J. Fish. Res. Bd. Can., 15, 115-134.

Miller, G.R., 1966: The flux of energy out of the deep oceans, J. Geophys. Res., 71(10), 2485-2489.

Swenson, E.M. and W.S. Brown and R. Trask, 1977: Great Bay Estuary Field Program, 1975 Data Report, Part I Currents and Sea Level, UNH Sea Grant Technical Report, UNH-SG-157.

Swift, M.R., R. Reichard and B. Celikkol, 1979: Stress and tidal current in a well-mixed estuary, J. Hydraul. Div., ASCE, 105, 785-799.

Taylor, G.I., 1919: Tidal friction in the Irish Sea, Phil. Trans. Roy. Soc. London, Ser. A, 220, 1-93.

APPENDIX A

THE ENERGY DISSIPATION CALCULATION

In order to use the correct version of Taylor's (1919) relationship for calculating the time averaged rate of energy flux into a bay passage there are several variables which require special discussion. One question which arises is what values of the long-channel velocity should be used. A single measurement at mid depth in the center of the channel would certainly not be representative of the entire cross-section. The way a section averaged current was estimated will be discussed below.

The long-channel component of the data collected during the profiling at each end of the study area was plotted on a cross-section of the channel at their respective locations. Each plot was made from the stations which comprised one cross-channel transect. The values were then hand contoured at 20 cm/sec intervals. An example of a typical cross-section from both ends of the study area is shown in figure 10. The area within each of the contours for a given transect was determined through the use of a planimeter. This area (m^2) was then multiplied by the average current speed (m/sec) within that contour to give a value of transport in m^3/sec. The transport for each of the contour sections were summed to give the total transport during a given transect. The time of the center station was the time assigned to the transport calculated for a particular transect. This procedure was followed for each succeeding channel transect. As a result a series of volume transport estimates over a complete M_2 (12.4 hours) tidal cycle were produced.

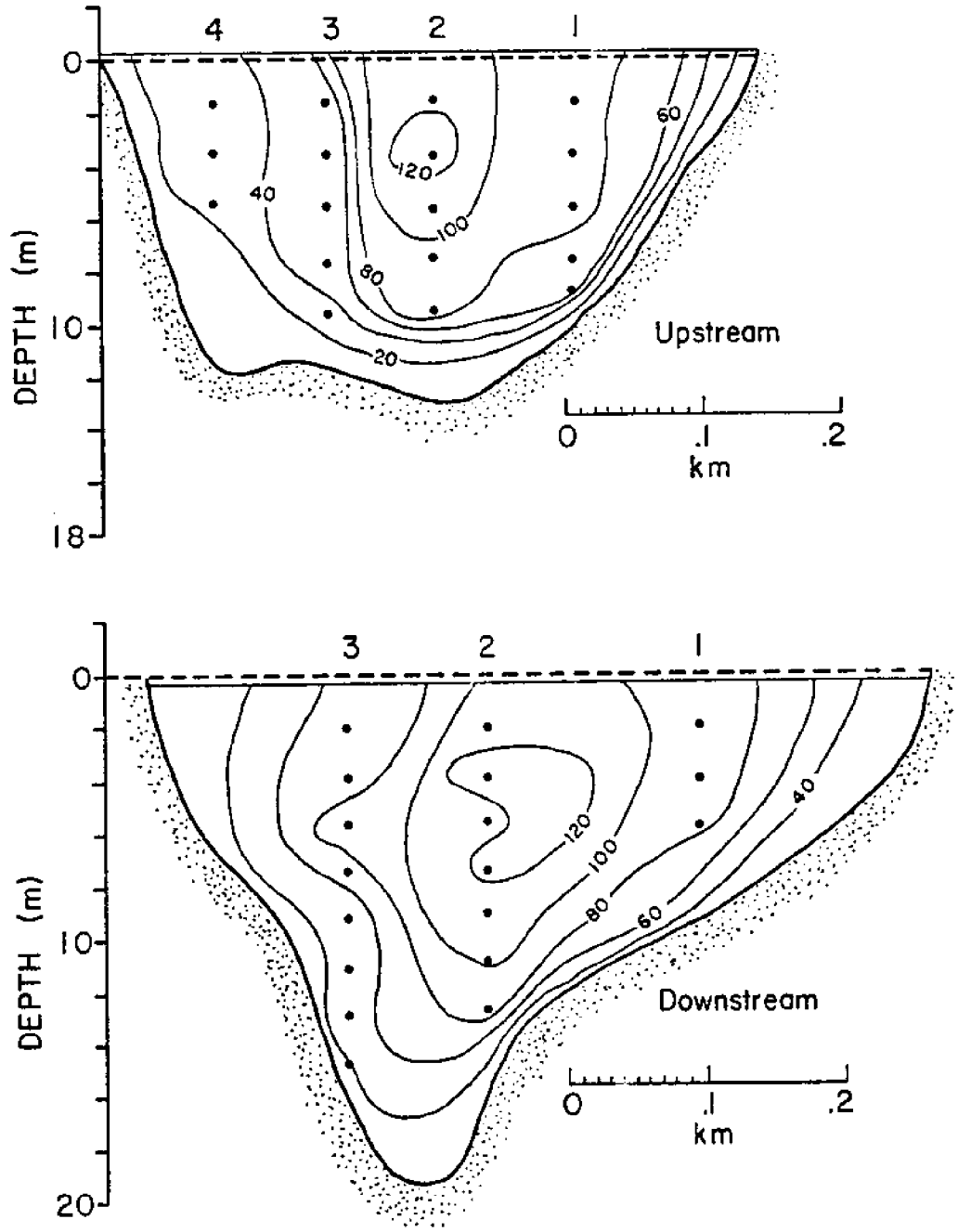

FIGURE 10. Typical cross-sections from both ends of the study area. Contour interval is 20 cm/sec, dashed horizontal line indicates mean low water, solid line indicates the water surface and (•) indicates the locations of current measurements. View is downstream. Positive flow corresponds to flow out of the estuary.

At the same time the current velocity profile data were being collected time series of currents were also being collected. Plots of current velocity and corresponding volume transports shown in figures 11 and 12 indicate that a linear relationship can be found with reasonable confidence. By applying the appropriate linear relationship to the time series of current speeds, a time series of volume transport, T, was created. A section averaged velocity, U, was calculated from the ratio of the volume transport at a particular time and the appropriate cross-sectional area.

Obviously the cross-sectional area of the channel fluctuates as the tide floods and ebbs. The cross-sectional area on the average increases by approximately 20% as the water rises from mean low water to mean high water. In order to develop a time series of cross-sectional areas needed in the above calculation the following procedure was used.

First the cross-sectional area of the channel below mean sea level was determined (a^2). Using that area and the width of the channel (w) a model channel with rectangular cross-section was constructed in which the depth below mean sea level (h) was constant.

$$h = \frac{a^2}{w} \qquad \text{(A-1)}$$

The calculated constant depth was then added to each member of a time series of sea level data (η_i). The newly created time series ($h + \eta_i$) was a record of the depth of the water in the rectangular channel. Each member of this time series was then multiplied by the channel width to get a time series of cross-sectional area.

$$(h + \eta_i)\ (w) = A_i \qquad \text{(A-2)}$$

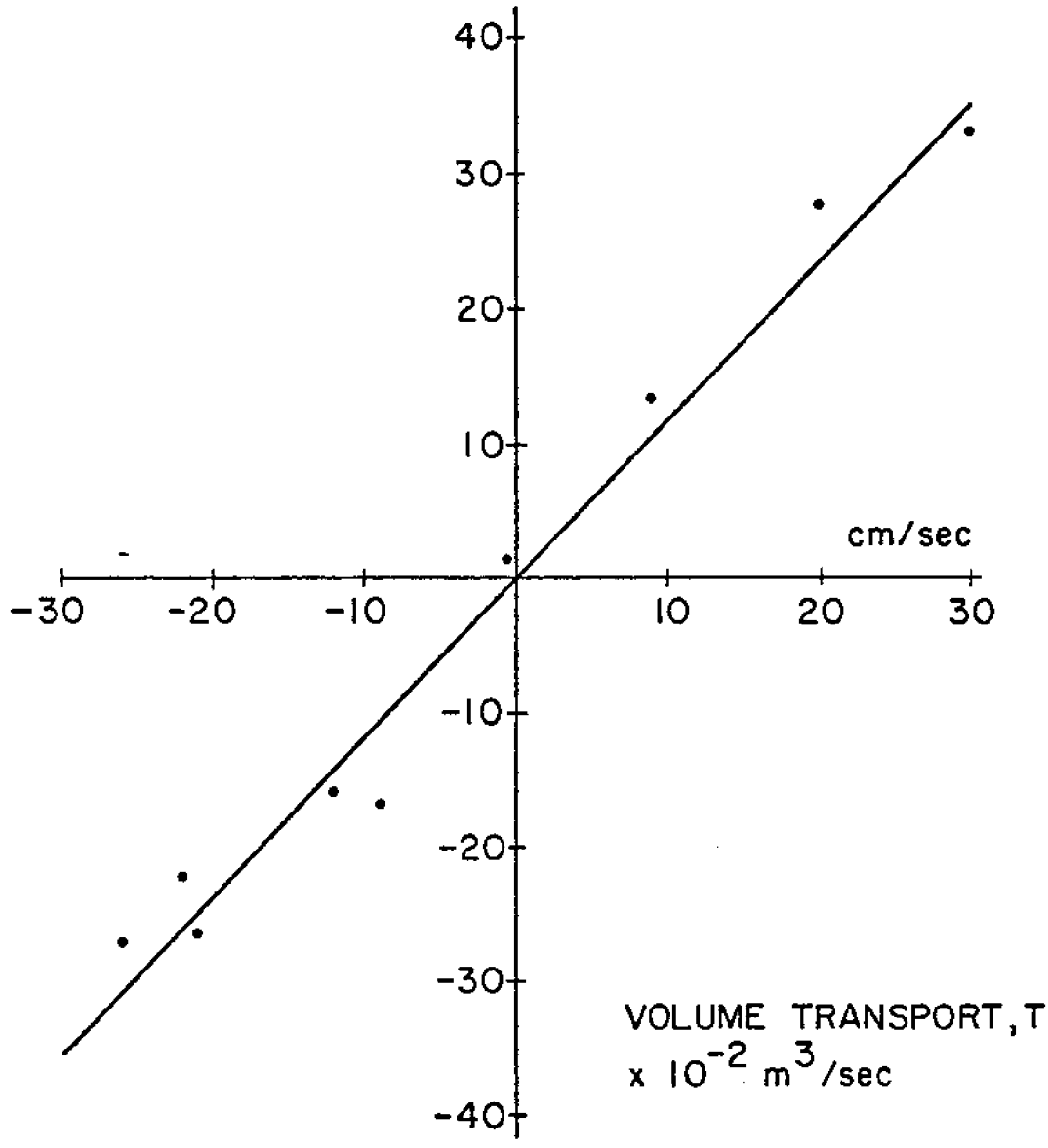

FIGURE 11. A plot of the long-channel component of current velocity versus volume transports from the upstream transect. The equation of the line which best fits the data is y = 116.9x with a corresponding r-square value of .975.

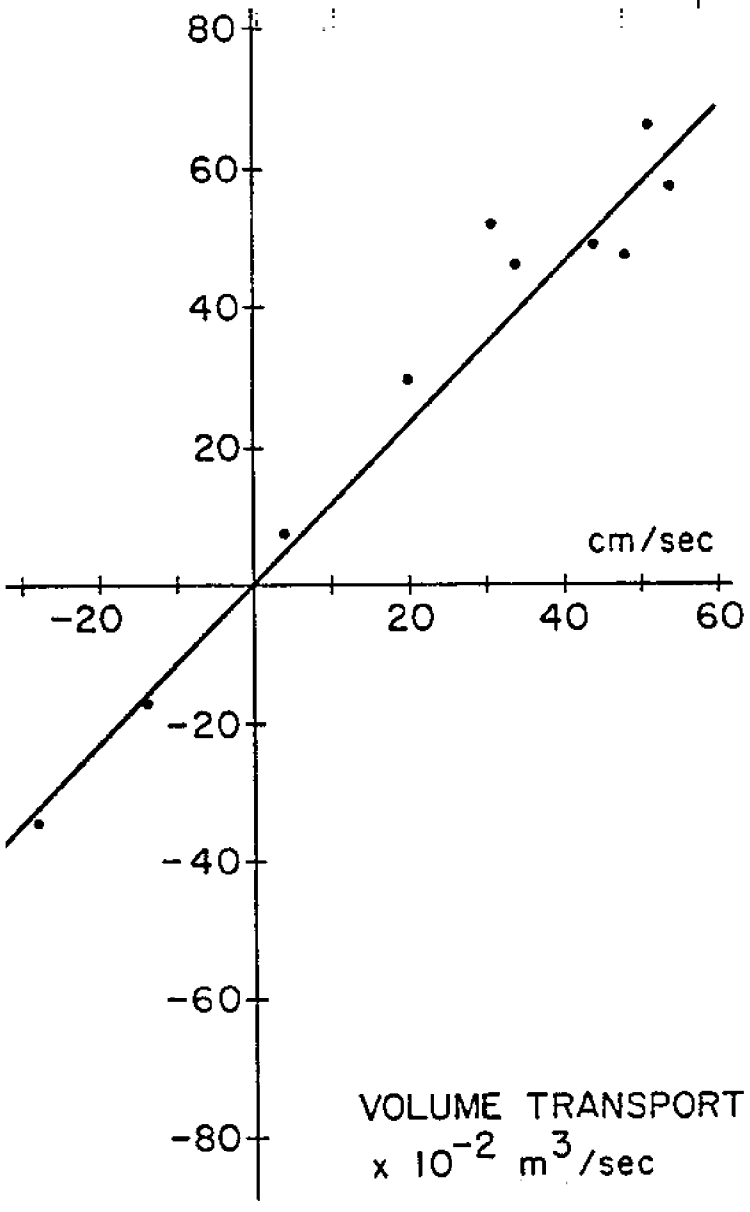

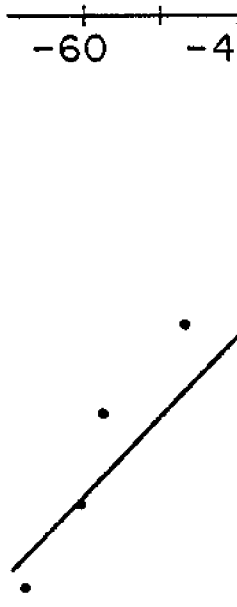

the long-channel component of current velocity
ts from the downstream transect. The equation
fits the data is y = 114.2x with a corresponding
.

FIGURE 12. A plot
versus volume tran
of the line which
r-square value of

The section averaged velocity U is therefore

$$U = \frac{T(t)}{A_i(t)} \qquad \text{(A-3)}$$

To calculate the energy flux through a particular cross-section of the channel the time series of sea level data (η_i) was multiplied by the section averaged velocity (U). The product was then multiplied by an appropriate constant density (ρ), a constant depth of the bottom below mean sea level (h), the width of the channel (w) and an acceleration due to gravity (g). The final product, ρ g U h η w, is a time series of energy flux values. An average of that time series was taken to give a value of the average energy flux for that particular location. A summary of the entire procedure can be found in figure 13.

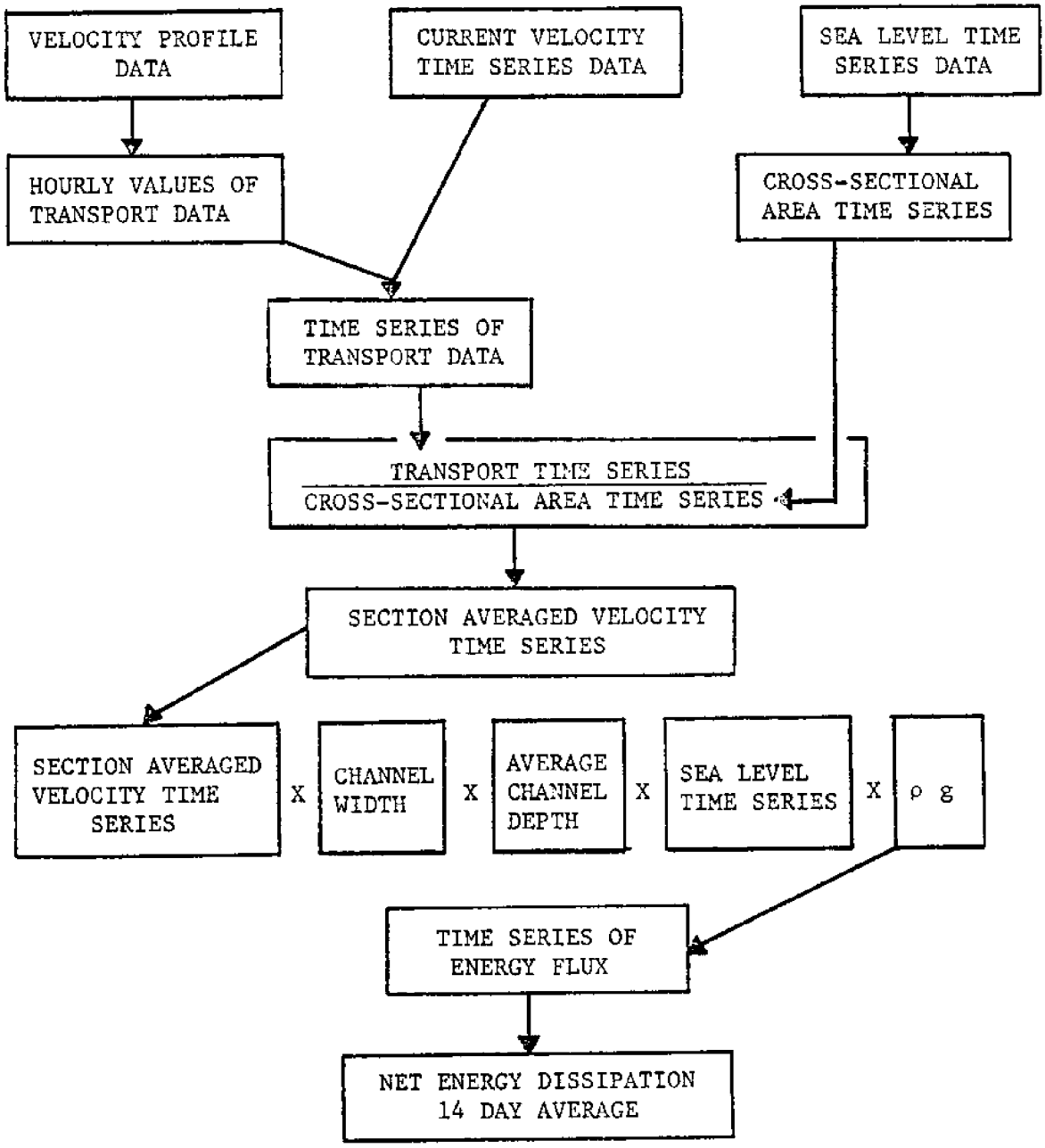

FIGURE 13. A summary of the procedure used to calculate the energy dissipation within the study area.

APPENDIX B

THE ENERGY DISSIPATION DUE TO VERTICAL MIXING CALCULATION

The calculation of the rate of energy dissipation due to vertical mixing required salinity and temperature profile data from the study area. One set of profiles that were used in the calculation were made near Frankfort Island and another set were made near the Schiller power plant. The salinity and temperature data were taken from Loder and Glibert (1977). Since the sampling at the two locations did not occur on the same day, the Schiller power plant data were adjusted so that the salinities and temperatures from both locations approximated synoptic data sets. Since more than one profile had been made at each location average salinity and temperature profiles were determined for each. From the temperature and salinity data water densities were calculated.

According to McLellan (1958) the equation for calculating the potential energy of a column of water of depth $(\eta + h)$ can be written:

$$PE = \int_0^{\eta + h} \rho \, g \, (h + z) \, dz \qquad \text{(B-1)}$$

where ρ is the density, g is the acceleration due to gravity and $(h + z)$ is the height measured from the bottom to the surface. To evaluate this function approximately using data taken at particular depths within the water column equation (B-1) may be rewritten as:

$$PE = \sum_0^{\eta + h} \bar{\rho} \, g \, (\overline{h + z}) \, \Delta z \qquad \text{(B-2)}$$

where $\bar{\rho}$ is the mean density of the water in the interval whose mean

height from the bottom is $(\overline{h + z})$. The convention followed in calculating the potential energy was to assume that a particular salinity value applied to the interval between the original depth of measurement and the next deeper depth of measurement.

Imagining a situation where fresh water of density ρ_f flows over water of uniform salinity S and density ρ_s with no mixing between the two layers, the potential energy of this ideal situation can be written:

$$(PE)' = (\overline{h + z_s})\ \Delta z_s\ \rho_s g + (\overline{h + z_f})\ \Delta z_f\ \rho_f g \qquad \text{(B-3)}$$

where Δz_s is the thickness of the salt water layer whose mean height is $(\overline{h + z_s})$ and Δz_f is the thickness of the fresh water layer whose mean height is $(\overline{h + z_f})$. After having selected a base salinity (S), i.e., the salinity of the ocean water, and calculating a depth averaged salinity $(\bar{S})$ for both profiles, the thickness of the salt water layer at each profile was calculated using:

$$\Delta z_s = \frac{\bar{S}}{S}\ (\eta + h) \qquad \text{(B-4)}$$

The thickness of the fresh water layer was therefore:

$$\Delta z_f = (\eta + h) - \Delta z_s \qquad \text{(B-5)}$$

The mean height of the salt water layer was:

$$(\overline{h + z_s}) = \frac{\Delta z_s}{2} \qquad \text{(B-6)}$$

and the mean height of the fresh water layer was:

$$(\overline{h + z_f}) = \Delta z_s + \frac{\Delta z_f}{2} \qquad \text{(B-7)}$$

The difference between the true potential energy (PE) and the ideal

potential energy (PE)' is a measure of the amount of energy per unit area which had been expended in producing the mixed state (ΔPE). The rate at which the energy was dissipated while mixing the fresh and salt water layers can be expressed as follows:

$$P_m = \frac{(\overline{\Delta PE})\ (A)}{T_m} \qquad \text{(B-8)}$$

where $\overline{\Delta PE}$ is the mean value of ΔPE over the area A which is being considered. T_m is the time in which mixing has taken place. An estimate of T_m was obtained by taking one-half the flushing time of the water in the area of interest. This represented an average time these waters were in the mixing mechanism.

Using equations (B-2) to (B-7) the average amount of energy per unit area expended to produce the mixed state in the study area was calculated to be 3.92×10^5 ergs/cm^2. To calculate the rate at which the energy was dissipated while mixing the fresh and salt water equation (B-8) was used along with an estimate of the time in which the mixing has taken place. According to Arellano (1978) the flushing time for a parcel of water at Frankfort Island is approximately three days to exit at the Portsmouth Harbor. Thus T_m in (B-8) is equal to 1.5 days since half the flushing time represents the average time these waters were in the mixing mechanism. The rate at which energy is dissipated due to vertical mixing was therefore calculated to be 5.02×10^{10} ergs/sec.

APPENDIX C

INSTRUMENT DEPLOYMENTS

The instrumentation associated with part two of the experiment included two pressure sensors and a Geodyne current meter. As described in chapter II the pressure sensors and a pressure housing which contained the electronics and data logging system were mounted on a rigid aluminium frame. Being aware of the strong tidal currents in the study area a heavy anchoring system was desired. In order to keep the pressure sensors in place each aluminium frame was attached to an 800 pound railroad wheel. The complete instrument package, which consisted of depth sensor, data logger, aluminium frame and weight was deployed from the R.V. Jere Chase. A surface buoy marked the location of the bottom instrument. The same line was used to deploy and retrieve the instrument package.

The Geodyne current meter was attached to an 800 pound tripod anchor frame shown in figure 14. The tripod frame was 2.5 meters tall and was weighted by a 600 pound railroad wheel. The whole tripod frame was stabilized by six one-meter long steel channels radiating from the center of the railroad wheel. Attached to the tripod frame was 1200 feet of 3/4 inch manilla rope. Once the current meter had been lowered to the bottom, the rope was slowly paid out as the R.V. Jere Chase steamed for the Maine side of the river. Once out of the channel the 3/4 inch manilla rope was attached to a 150 pound satellite mooring which also had a lighter line attached to it with a buoy at the surface. This was done to avoid interference with normal river traffic and per-

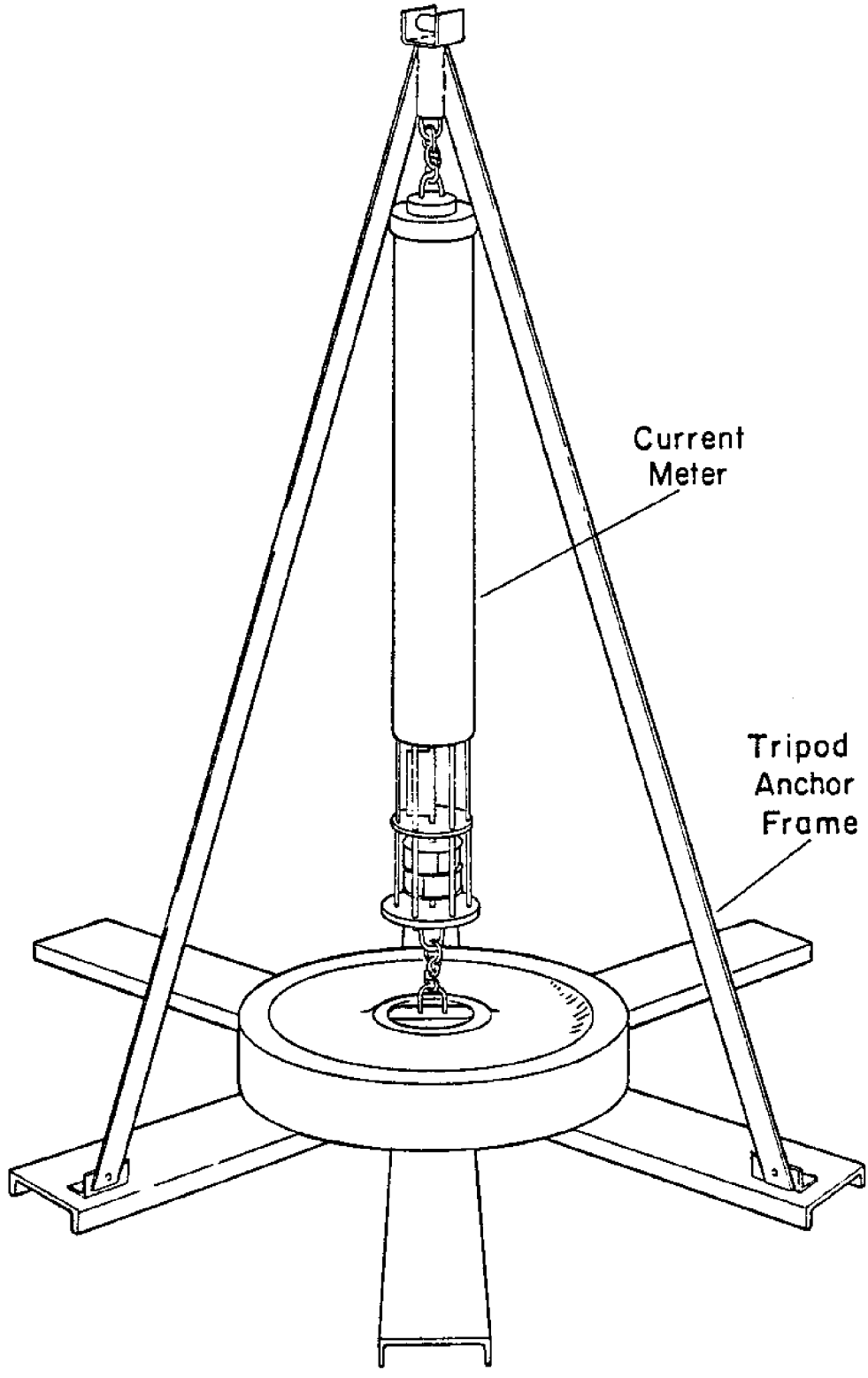

FIGURE 14. A schematic drawing of the tripod anchor frame used to secure the Geodyne current meter in the center of the channel.

mitted a relatively easy retrieval of the current meter without the use of divers. The configuration of the instruments on the bottom is shown in figure 15.

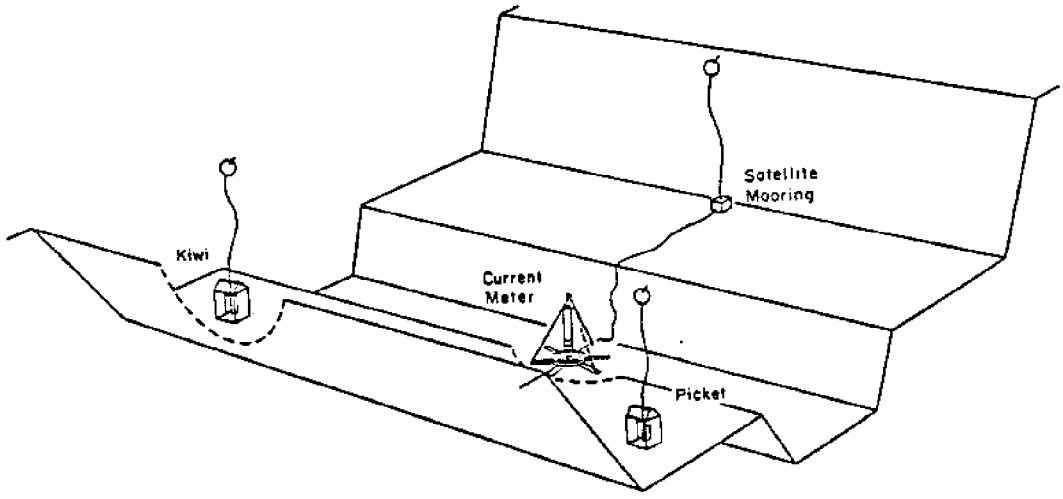

FIGURE 15. A schematic drawing of the locations of the two pressure sensors at each end of the study area and the Geodyne current meter in the center of the channel.

APPENDIX D

UNCERTAINTY ESTIMATES

Uncertainties related to calculations made in part one of the experiment stem from several sources. There is the problem of missing part of the flow during the transects, instrument uncertainty and data reduction uncertainties. The problem of missing part of the volume transport is related to the actual sampling procedure and its limitations. The positions of the stations during the current transects was one reason for missing part of the flow. An example of a typical cross-section from both ends of the study area is shown in figure 10. In the case of the downstream transect the bathymetry of the channel was such that stations two and three were on either side of a very deep portion of the channel. The near bottom current measurements made at these two stations are likely to have been within the boundary layer thus giving low velocities while the center of the channel may have still been flowing at a much higher velocity. To estimate the volume transport that was undetected the cross-sectional area of the region which was lacking data was multiplied by the difference between what is believed to be a true estimate of the velocity in that area and the velocity actually used in the original transport calculation. That undetected volume transport was then compared with the total volume transport calculated for that transect. The calculated volume transport was found to be underestimated by 8% (BU1, Biased Uncertainty) because of the missing deep channel data. This was found to be true for maximum and average flow conditions. A similar problem occurred toward the end of the upstream transect where the depth to which

current measurements could be made was limited to about ten meters. Whenever deeper measurements were attempted a considerable amount of noise began to be introduced into the signal. The volume transport, undetected because of the measurement limitations, was estimated the same way as above and was found to be approximately 6% (BU2) of the original volume transport.

In addition to the near bottom measurements the current measurements near the flanks of the channel were also lacking. Using the same procedure as described earlier it was found that the volume transports were underestimated by 5% (BU3) due to sparse data near the sides of the channel.

The four station sampling routine used at the upstream transect is believed to have underestimated the total volume transport. The four stations were sampled in the following order, 1, 2, 3, 4, 1, 2, 3, 4 and so on. It obviously took more time to make a complete transect using the four station routine than it did using three stations which were sampled 1, 2, 3, 2, 1, 2, 3 and so on at the downstream transect. A complete transect took approximately 1.5 hours using four stations whereas the three station routine only took about one hour. Using the volume transport curve from the downstream transect (~1 hour between values) volume transport values corresponding to every 1.5 hours were taken from the curve and plotted on a separate graph. The total volume transport calculated with the 1.5 hour sampling rate underestimated the total transport calculated using hourly values by 6% (BU4) due to non-synoptic measurements.

Another possible source of error is that introduced by instrument uncertainty. During the course of the experiment the electromagnetic

current meter often indicated incorrect current directions as well as recorded several periods of noisy current velocity data. The periods of current meter malfunction were more frequent during the upstream transect than during the downstream transect. The uncertainty of this instrument based on the manufacturers specifications is ±2% (RU1, Random Uncertainty). The technical manual for the Geodyne current meter model 102 suggests that the accuracy of that instrument is ±5% (RU2) provided the velocity is under 51.5 cm/sec which it was since the rotor was only 75 centimeters from the bottom.

Another source of uncertainty is that introduced by the data reduction procedures which are described in Appendix A. One operation in the data analysis requires the current transect data to be hand contoured. An estimate of the error introduced by the contouring procedure was made by several students of a physical oceanography class. In one analysis contouring the same data several different ways showed that the uncertainty introduced was on the average ±11%. This uncertainty, however, is in part related to the problem of sparse current velocity data. In the analysis of that uncertainty, estimates of more realistic contours were made to determine which part of the flow was going undetected. Thus included with the uncertainty estimates of missing flow is the uncertainty of the contouring procedure. Planimetering the contoured data is another source of uncertainty which could be introduced by the data analysis. To estimate that error the same contours were planimetered by two different people. The results showed that the uncertainty of the planimetering process was ±5% (RU3).

It appears that the transports from both ends of the study area have been underestimated. The biased uncertainty could not for the

downstream transports is:

$$(BU1 + BU3) = (8\% + 5\%) = 13\%$$

while for the upstream transports it is:

$$(BU2 + BU3 + BU4) = (6\% + 5\% + 6\%) = 17\%.$$

It is believed that the downstream and upstream transports have been underestimated by approximately 13% and 17% respectively; however, these are only estimates of the biased uncertainty. The random error associated with these estimates of the biased uncertainties is believed to be ±5% (RU4). The random errors of the electromagnetic current meter and the planimetering procedures effect the transports at each end in the same manner. Thus the random error associated with the transport calculation is:

$$((RU1)^2 + (RU3)^2 + (RU4)^2)^{1/2} = ((\pm 2\%)^2 + (\pm 5\%)^2 + (\pm 5\%)^2)^{1/2} = \pm 7.3\%$$

Due to the data analysis procedures outlined in chapter I the uncertainty of the transports can produce uncertainties in the bottom stress calculation which are far greater than the uncertainty introduced by the Geodyne current meter. The uncertainty in the final bottom stress calculation cannot be determined in general but rather depends on the data analysis procedures which require a relationship between the volume transports and a centrally located current measurement.

The uncertainties associated with part two of the experiment fall into three categories, those related to instrument uncertainty, those which are related to the assumptions made in the original theory and those related to the prediction procedures. The uncertainties related

to the instruments used in part two of the experiment will be discussed first. According to the manufacturers specifications the Digiquartz pressure sensors have an overall precision of better than .01% (RU5). The Geodyne current meter as stated earlier has an uncertainty of ±5% (RU2).

Another source of uncertainty is related to an assumption made in order to reduce the integrated long-wave momentum and continuity equations to the form shown in (8). That assumption was that the downstream variations in current velocity were zero ($\delta U/\delta x = 0$). If this were so the contribution of the term $U(\delta U/\delta x)$ in the long-wave momentum equation would be zero. For four locations in the study area an average velocity was calculated using an estimate of the volume of water passing each location, the cross-section of the channel at each location and a half tidal cycle period of 6 hours and 12 minutes. On the average the velocities varied from the mean by about 5 cm/sec. The distance between the four locations was determined and the contribution of $U(\delta U/\delta x)$ was calculated to be 5.5×10^{-3} cm/sec^2. Compared to the major contribution of $g(\delta \eta/\delta x)$ the uncertainty introduced by not including $U(\delta U/\delta x)$ in (8) is ±10% (RU6). Thus the overall uncertainty in the bottom stress calculation utilizing all real data is:

$$((RU5)^2 + (RU2)^2 + (RU6)^2)^{1/2} = ((\pm.01\%)^2 + (\pm5\%)^2 + (\pm10\%)^2)^{1/2} = \pm11.2\%$$

Those bottom stress calculations made using predicted series have an additional uncertainty related to the predictions. The predicted series are at best only as good as the data used to determine the harmonic constants. Assuming that the data represents sea level fluctuations due solely to the tides an analysis of the variance of the data

and of a predicted series shows that for the Atlantic Terminal tide station the prediction represents 96.3% of the sea level fluctuations observed by the original data, at the Simplex location the prediction includes 97.6% of the observed tidal oscillations and for the Schiller Plant location the prediction represents 96.7% of the observed sea level fluctuations. Taking the worst case the uncertainty introduced by using predicted sea level series is about 3.7% (RU7). Thus the total uncertainty in the bottom stress calculation utilizing predicted time series is:

$$((RU2)^2 + (RU6)^2 + (RU7)^2)^{1/2} = ((\pm 5\%)^2 + (\pm 10\%)^2 + (\pm 3.7\%)^2)^{1/2} = \pm 11.8\%$$

APPENDIX E - Characteristic Velocity Calculation

An area-averaged value of bottom stress can be estimated from a known value of frictional dissipation and average velocity for a region of an estuary. The average velocity in the study area was estimated by two methods. The first method combined the profile data and the Geodyne current meter data from the center of the study region in order to estimate a vertically averaged velocity. The second method used the transport data from each end of the study area in order to obtain a section-averaged velocity. A more detailed description of each method and their results will follow.

The first method for estimating an average velocity required simultaneous Geodyne current meter data and profile data. The current profiles shown in figure 16 were integrated to obtain an estimate of a depth-averaged current velocity. The mean time of the profile was assigned to the depth-averaged velocity estimate. Unfortunately the Geodyne current meter was not recording data at the time the profiles were made. We addressed this problem by performing a tidal analysis of the Geodyne current meter data with a computer program used by NOS as outlined by Dennis and Long (1971). The harmonic constants were used to predict a long-channel current for the time period which coincided with the profile data. A comparison shown in figure 17 was then made between the vertically averaged velocities obtained from the profiles and the predicted Geodyne velocities. Since the rotor of the Geodyne current meter was within the bottom boundary layer the values were systematically lower than our estimates of depth-averaged velocity. A linear approximation to this relation (shown in figure 17) was used to convert current meter observations into a depth average velocity series. This was done to a 14-day time series of Geodyne

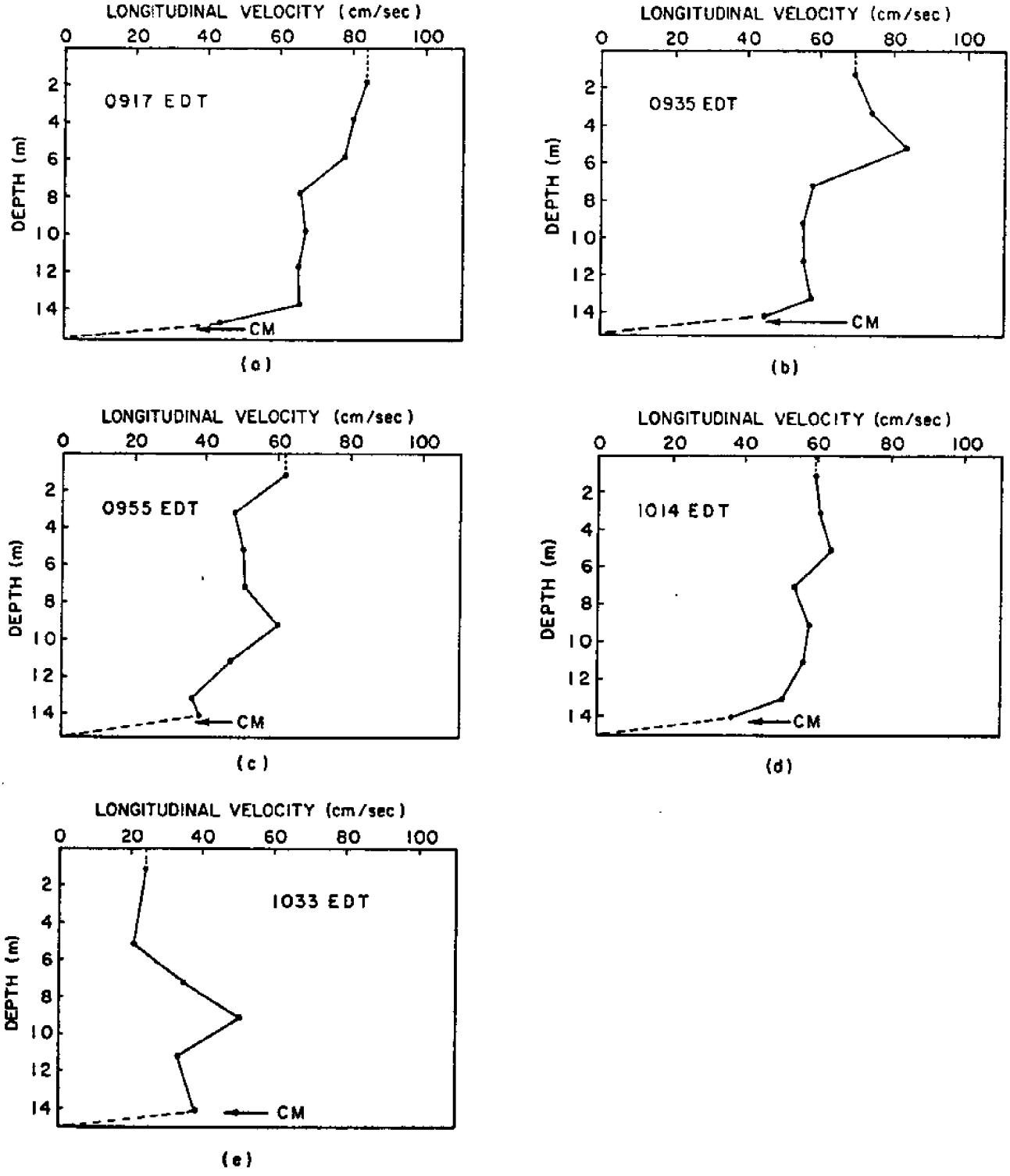

Figure 16 - A sequence of current profiles measured near the Geodyne current meter on 21 September 1978 (a) 0917, (b) 0935, (c) 0955, (d) 1014 and (e) 1033 EDT respectively. The depths are referenced to sea-level with the current meter elevation as indicated within the bottom boundary layer.

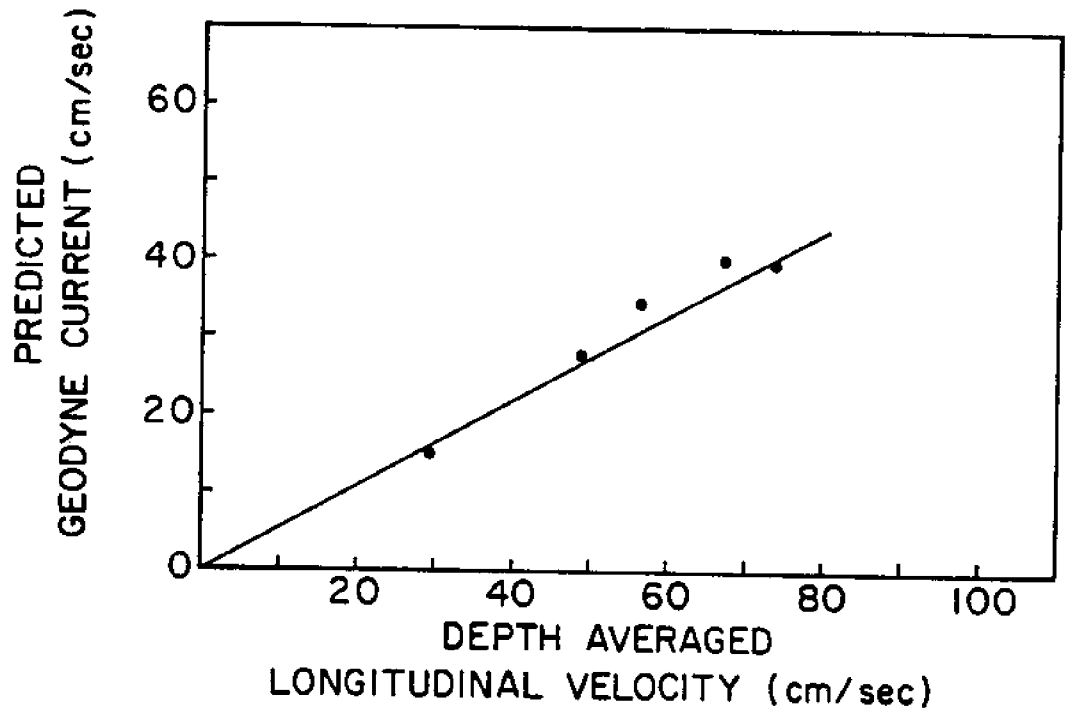

Figure 17 - A comparison of depth averaged velocity from current profile measurements (see figure 16) and the predicted bottom currents based on the tidal analysis of the Geodyne currents.

currents to produce a time series of vertically averaged currents. The RMS value of a 14-day vertically-averaged current at the center of the study area was 57.64 cm/sec.

The second method for estimating an average velocity used the section-averaged velocities calculated from the transport estimates obtained at each end of the study region. A detailed discussion of how these time series were created is described in Appendix I. The 14-day velocity time series from each end of the study area were averaged to obtain a representative section-averaged velocity time series for the area of interest. The RMS value of this result was 65.05 cm/sec.

Since the two methods yielded slightly different results an average of the two values was taken. The resulting average velocity used in the energy dissipation method for calculating an average bottom stress was 61.34 cm/sec.

APPENDIX F - Tidal Prism Volume Determination

An estimate of the tidal prism volume distribution is useful for evaluating the accuracy of volume transport estimates made at specific locations within an estuary. A tidal prism volume distribution estimate for the Great Bay Estuary has been determined on the basis of the Coast and Geodetic Survey Chart 212 (new number?). The estuary has been divided into several sections shown in figure 18. Accordingly the tidal prism volume of each section has been determined. A planimeter was used to determine the water surface area at high and low water for each section. A mean tidal range of 2 m (based on the sea level distribution in the Great Bay Estuary as shown by Swenson, Brown, and Trask (1977)) was assumed for the calculation. To account for tidal flats we also assumed that the topography of the tidal flat area between mean low and high water is smooth and featureless so that the tidal prism of the estuary can be schematically represented as shown in figure 19. Multiplying the tidal range by one-half the difference between high and low water areas gives the volume of water which occupies the region over the tidal flat area at high water. Adding this volume to the product of the low water area and the tidal range gives an estimate of the total tidal prism volume. The tidal prism obtained by applying this method to the Great Bay Estuary was 80.53×10^6 m^3. In table 4 the high and low water areas are summarized along with the corresponding section estimates of the tidal prism.

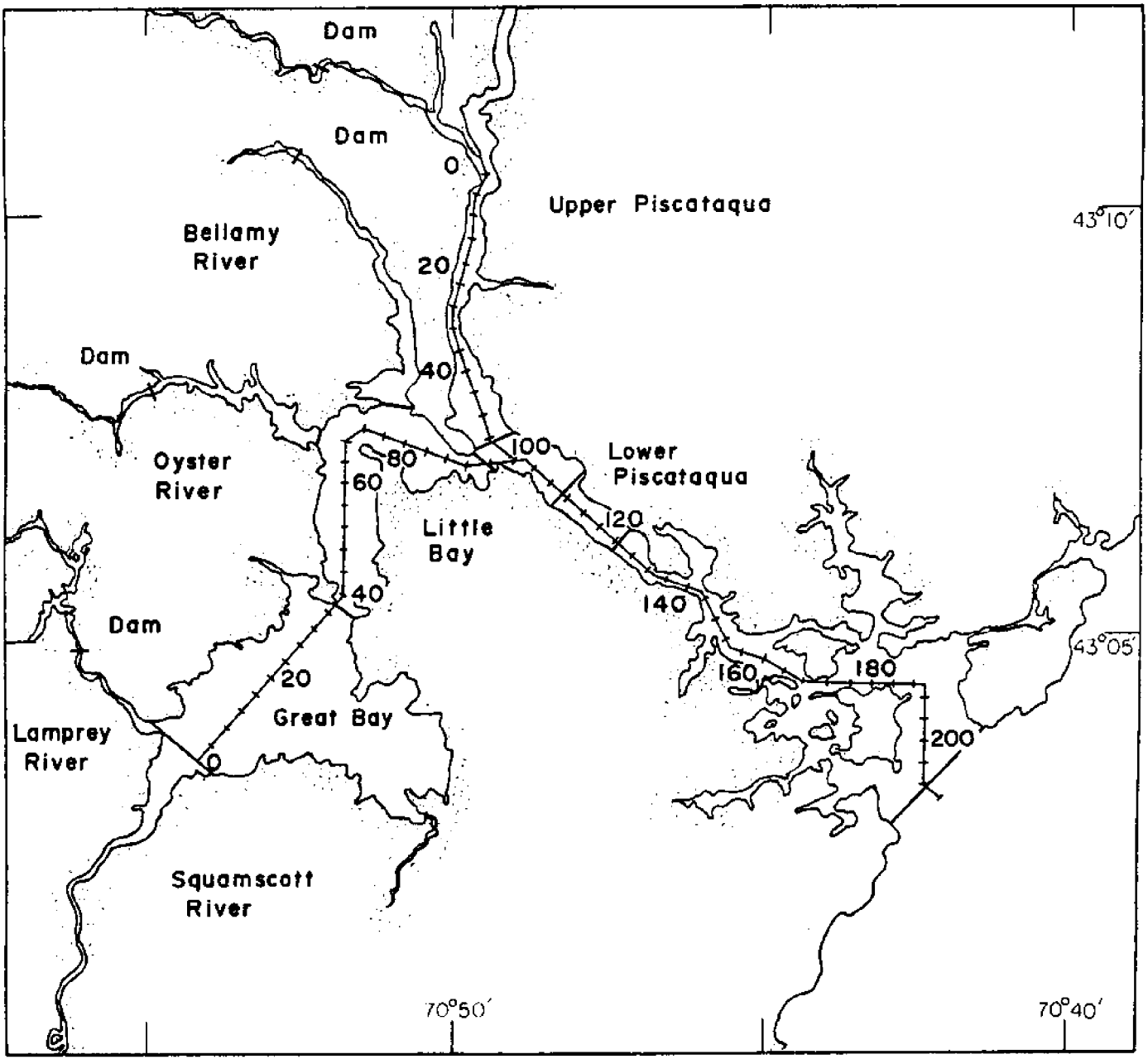

Figure 18 - The Great Bay Estuary with the longitudinal estuarine scale. The main branch begins at the junction of the Lamprey and Squamscott Rivers and ends at the entrance to Portsmouth Harbor. The secondary branch begins at the Cocheco and Salmon Falls River and terminates at the junction between the Upper and Lower Piscataqua. The scale is 8 units per kilometer. The dark lines crossing parts of the estuary indicate the sections where tidal prism volumes were determined individually. Those volumes appear in table 4.

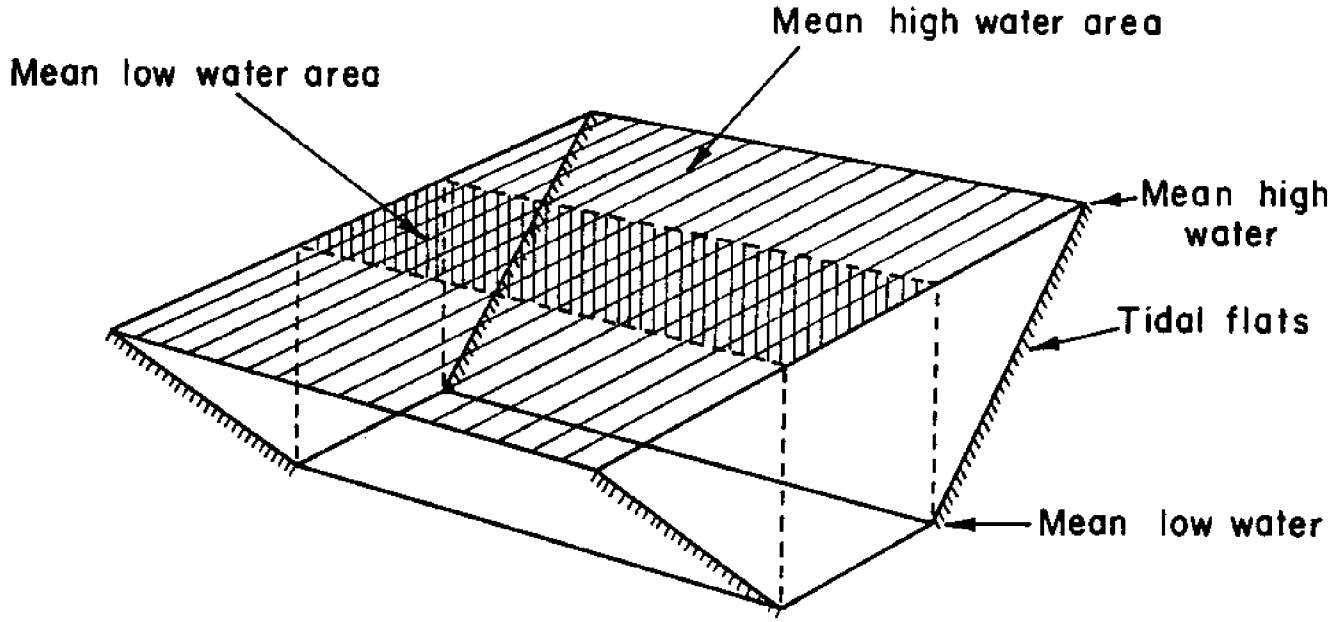

Figure 19 - Schematic representation of a tidal prism volume in an estuary.

Section	High Water Area $(Km)^2$	Low Water Area $(Km)^2$	Prism Volume $(10^{-6}m^3)$ (Trask)	(Arellano)
Great Bay				
Squamscott R., Dam to 0	3.65	.94	4.59	
Lamprey R., Dam to 0	.27	.16	.54	
0 to 38	16.96	7.17	24.13	18.81
			29.26	
Little Bay				
38 to 95	7.66	5.24	12.90	15.75
Oyster R., Dam to Mouth	1.82	1.00	2.82	
Bellamy R., Dam to Mouth	1.85	.62	2.46	
			18.19	
Upper Piscataqua				(0-60)
Dams to 64	5.48	2.69	8.17	6.14
			8.17	
Lower Piscataqua				
95 to 111	1.88	1.48	3.36	
111 to 125	1.00	.89	1.89	
125 to 209	10.61	9.05	19.66	
			24.91	24.46
Total	51.18	29.24	80.53	63.64

Table 4. A summary of the high and low water areas and the calculated volumes. The numbers describing particular sections refer to the estuarine scale shown in figure 18.